



# NAVAL RESEARCH LABORATORY REPORT

1 December 1946

SIGNAL THRESHOLD STUDIES

By  
R. M. Ashby, V. Josephson  
S. Sydorak

Report R-3007

APPROVED FOR PUBLIC  
RELEASE - DISTRIBUTION  
UNLIMITED

NAVY DEPARTMENT  
OFFICE OF NAVAL RESEARCH  
NAVAL RESEARCH LABORATORY  
WASHINGTON 20, D. C.

NAVAL RESEARCH LABORATORY  
Washington, D. C.

\* \* \*

NAVAL RESEARCH LABORATORY FIELD STATION

---

1 December 1946

SIGNAL THRESHOLD STUDIES

By R. M. Ashby, V. Josephson, S. Sydorjak

- Report R-3007 -

UNCLASSIFIED

\* \* \*

Approved by:

H. Krutter - Chief Scientist NRLFS, Boston, Mass.

Comdr. W. E. Bostwick  
Officer-in-Charge  
NRLFS, Boston, Mass.

Commodore H. A. Schade  
Director, Naval Research Laboratory  
Washington, D. C.

---

Preliminary Pages ..... 2 - 0  
Numbered Pages ..... 30  
Figures ..... 1 - 26

### Credit for this Report

The experimental work that formed the basis of this report was done by Group 44 at Radiation Laboratory, Massachusetts Institute of Technology. The original plans called for this report to be issued as Radiation Laboratory report number 915. It was not possible to complete the preparation until too late for publication by that agency.

In view of the general value of the information, and in particular its value to the Cadillac Project, permission was obtained to have the report published by the Naval Research Laboratory Field Station, Boston, Massachusetts.

In Group 44 of Radiation Laboratory, the following personnel worked on this project: C. M. Allred, R. M. Ashby, A. L. Gardner, Dorothy Gillette, V. Josephson, J. L. Lawson, F. W. Martin, R. R. Meijer, E. R. Shepherd, S. G. Sydoriak, and F. D. Williams.

One of the authors of this report, R. M. Ashby, is now a member of this station, and is extending the investigation of this project here.

### Abstract

Extensive laboratory tests have been carried out to determine the effect of the different radar-system parameters on the minimum pulse power detectable in receiver noise. The results are reported in the form of graphs with brief explanations of each as well as the theory involved. The tests were carried out using an A-scope and a PPI as indicating instruments.

The parameters which were investigated using the A-scope type of indicator are as follows: Pulse repetition frequency, signal presentation time, I-f and video bandwidth, sweep speed, extra noise sweeps, integration effect of P1 and P7 screens, focus, trace intensity, receiver gain.

The parameters investigated on the PPI are as follows: Pulse repetition frequency, I-f bandwidth, random possible azimuths, per cent of signal overlap on successive scans, scanning speed, and dependence on signal angular arc.

In every case, the signal threshold power is given in terms of the receiver noise power, and consequently the power in watts required for signal detection for any set of conditions reported can easily be calculated for any receiver of known noise figure.

The values of signal threshold  $S_{90}$  given, represent the signal power required for an observer to name the correct position out of six, 90 per cent of the time (the signal having equal probability of being at any one position). All tests were carried out under carefully controlled conditions so that adequate checking of results could be obtained.

TABLE OF CONTENTS

TITLE PAGE.....	a
CREDIT FOR REPORT.....	b
ABSTRACT.....	c
TABLE OF CONTENTS.....	d.
I. INTRODUCTION.....	1
II. FACTORS INVOLVED IN THRESHOLD MEASUREMENTS.....	1
A. Systems Parameters.....	1
B. Definition of Signal Threshold Power.....	2
C. Theoretical Approach.....	3
D. Signal Power, S, Measured Relative to Receiver Noise Power N.....	6
E. Scaling.....	6
III. EXPERIMENTAL PROCEDURE.....	7
A. Apparatus.....	7
B. Techniques.....	10
IV. EXPERIMENTAL RESULTS ON A-SCOPE.....	17
A. Statistical Effects.....	17
B. Geometrical Parameters.....	25
C. Contrast Effects.....	25
V. SIGNAL THRESHOLD MEASUREMENTS ON PPI.....	26
A. PRF.....	26
B. Signal Presentation Time, T.....	26
C. The Effect of the Variation of the Product of I-f Bandwidth and Pulse Length on the Signal Threshold Power.....	27
D. Random Possible Signal Azimuths.....	27
E. Overlap.....	28
F. Dependence on Angular Arc.....	29
G. Equation for Estimating Scanning Loss.....	29
APPENDIX I THEORETICAL BETTING CURVES FOR AN OBSERVER WITH AN AVERAGING DEFECT.....	34
A. Definition of Contrast and Averaging Defect.....	34
B. Uhlenbeck's Theoretical Relations.....	35
C. Betting Curve Calculations for the Two-position Experiment	36
D. Betting Curve Calculations for the Six-position Experiment	37
FIG. 1. Some Betting Curves of A-scope Experiments	
FIG. 2. Probability Distribution of Amplitude, $X$ , for a Linear Detector for Noise, and for Noise Plus Signal	
FIG. 3. Block Diagram of the System used for Threshold Studies	
FIG. 4. Signal Threshold Power Vs. PRF	
FIG. 5. Signal Threshold Vs. Signal Presentation Time	
FIG. 6. Signal Threshold Vs. Pulse Recurrence Frequency with Sweep Recurrence Frequency Constant at 3000/sec	

TABLE OF CONTENTS (cont'd)

- FIG. 7. Signal Threshold Vs. Sweep Recurrence Frequency, SRF, with Sweeps Containing Signal Pulse Constant at 200 per sec.
- FIG. 8. Signal Threshold Vs. Number of Possible Signal Positions
- FIG. 9. Signal Threshold Vs. Attention Interval, with Signal Presentation Time Constant 0.1 sec.
- FIG. 10. Signal Threshold Power Vs. I.F. Bandwidth X Pulse Length
- FIG. 11. Signal Threshold Vs. Video Bandwidth for Fast and Slow Sweeps
- FIG. 12. Signal Threshold Vs. Pulse Length on Screen
- FIG. 13. Signal Threshold Vs. Focus
- FIG. 14. Signal Threshold Vs. Receiver Gain
- FIG. 15. Signal Threshold Vs. Trace Intensity
- FIG. 16. Deviations from the Threshold of Uhlenbeck's Ideal Observer
- FIG. 17. Twilight Zone Vs. Number of Signal Pulses
- FIG. 18. Probability of Coincident Misses in a 6-Position 2-Observer Experiment
- FIG. 19. Theoretical Betting Curves for 3, 80, and 800 Signal Pulses and Various Assumed Values of the Averaging Defect,  $\delta$ , of the Observer
- FIG. 20. Signal Threshold Vs. Pulse Repetition Frequency on PPI
- FIG. 21. Signal Threshold Vs. Signal Presentation Time with Scanning-Time Constant
- FIG. 22. Signal Threshold Power Vs. I-F Bandwidth X Pulse Length on PPI
- FIG. 23. Scanning Loss as a Function of the Per Cent of Signal Overlap
- FIG. 24. Scanning Loss as a Function of Scanning Rate
- FIG. 25. Signal Threshold Vs. Scanning Time With Signal Presentation Time Constant
- FIG.A-1 Scheme for Calculating the Letting Curve for an Observer with Limited Contrast Discernibility; i.e., Having a Finite Averaging Defect,  $\delta$ .

## SIGNAL THRESHOLD STUDIES

### I. INTRODUCTION

It was the purpose of this study to investigate the signal power needed for detection of a radar echo. At the time this problem was undertaken, it was clear that many systems parameters influenced the threshold power required. At about that time Haeff of NRL and others since, both in U.S. and abroad, have reported similar studies, however, of less general scope.

### II. FACTORS INVOLVED IN THRESHOLD MEASUREMENTS.

#### A. Systems Parameters.

From the beginning a list was made of those parameters which might influence the signal threshold power. While this list is admittedly incomplete, and may also include some parameters having small significance, it is included here to aid in orientation in regard to the parameters which were investigated and those that were not.

#### Systems Parameters Possibly Influencing Signal Threshold Power

- |  |   |
|--|---|
| 1. Pulse length $\mu$ sec.   | 10. Scope trace intensity.                                  |
| 2. I-f bandwidth, B Mc/sec   | 11. Scope focus.  |
| 3. Type of i-f circuit.<br>(Single or multiple tuned)<br>(Single or multiple narrowed) | 12. Ambient light.  |
| 4. Video bandwidth, b Mc/sec.  | 13. Receiver gain db.                                       |
| 5. Type of video circuit - frequency<br>and phase response                             | 14. Signal presentation time, T sec.                        |
| 6. Pulse Repetition Frequency, PRF<br>pulses/sec.                                      | 15. Attention interval -- signals<br>random in time T' sec. |
| 7. Sweep rate, mm/ $\mu$ sec.  | 16. Various operators scatter.                              |
| 8. Law of second detector and video<br>amplifier.                                      | 17. Degree of FM on pulse.                                  |
| 9. Type of scope screen P <sub>1</sub> , P <sub>7</sub> .                              | 18. Variability of signals.                                 |
|  | 19. Number of signal positions.                             |
|  | 20. Signal arc on PPI, degrees.                             |

21. Scanning rate, rev/min.
22. Extra noise sweeps -- sweep recurrence frequency  $SRF_e$ , sec.
23. Direction of sweep, horizontal or vertical.

It was determined to vary one (if possible) of these parameters, and investigate the way the signal threshold power varied.

B. Definition of Signal Threshold Power.

Perhaps the most difficult aspect of the problem in the beginning was in finding a suitable criterion for a threshold signal. Many different criteria were tried but most of these had psychological factors involved which were not too well reproducible from observer to observer nor for the same observer over a period of time. The elimination of these psychological factors was largely accomplished by the adoption of a purely statistical criterion, which has been further developed by Uhlenbeck, Wang, and others.

Several discrete positions (discrete values of range)<sup>(1)</sup> were marked on the face of the indicator tube, either A-scope or PPI. Each one of these had equal (random) probability of being the signal position. The observer was instructed to give the position where the average deflection<sup>(2)</sup> (or intensity) was greatest as the signal position. The correlation above chance between the actual signal positions and those named by the observer was plotted as a function of signal power,  $S$ . Figure 1 gives examples. The signal power for which this correlation is 90% has arbitrarily been taken as the signal threshold power, written  $S_{90}$ . A signal power having any other percentage correlation was designated by the corresponding subscript; 50%,  $S_{50}$ , etc.

---

(1) Except for the influence of memory and the difficulty of designating them, points in time could equally well be used. Theoretically they are the same.

(2) Actually for best results the average power should be taken.

### C. Theoretical Approach.

For simplicity the two-position, single-sweep experiment is considered. Suppose the signal is at position  $z$ . Then the probability distribution of the amplitude at the other position,  $y$ , is given by the curve  $\lambda = 0$  in Fig. 2.<sup>(3)</sup> This is the amplitude probability distribution for noise as it comes from a linear detector. At position  $z$ , where the signal is, the amplitude probability distribution will depend on the signal power and may be given by any one of the curves in Fig. 2. The parameter  $\lambda$  is a measure of the signal power.

If the signal power is so low that the curve  $\lambda = 0$  applies closely also to the signal position,  $z$ , and if the observer reports the higher position each sweep, for a large number of sweeps, position  $z$  will be reported just one half of the times, which is just chance. The probability that the signal position will be lower than position  $y$  is equal to one half the area  $A$  common to both curves ( $A$  is cross hatched in Fig. 2 for  $\lambda = 4$ , signal power 4 times noise).

$$P_{z < y} = \frac{A}{2} \quad (1)$$

The probability that the signal position,  $z$ , is higher, is of course:

$$P_{z > y} = 1 - P_{z < y} = 1 - \frac{A}{2} = \frac{B}{2} + \frac{A}{2} \quad (2)$$

where  $B$  is the remaining area under both curves. (The curves are each, of course, normalized to a total area of unity).

One half the area under both curves not shared,  $\frac{B}{2}$ , is then the probability above chance that the signal position has greater amplitude than the noise position. If this probability or correlation above chance is computed and plotted as a function of signal power a theoretical curve corresponding to the experimental curves of Fig. 1 is obtained, from

---

(3) Figure 2 is taken from North, RCA Report PR-600, Sheet 34.

which the theoretical signal threshold power  $S_{90}$  can be obtained and compared with the experimental results.

This type of theoretical computation of signal thresholds can be extended to any number of positions and any number of signal sweeps. For this computation reference should be made to Uhlenbeck's discussion in the Radiation Laboratory Technical Series<sup>(4)</sup> A special application of the general method was used in Appendix A of this report but for the present, it can be stated that the curves corresponding to those of Fig. 2, but computed for  $n$  averaged sweeps, approach Gaussian shape in either voltage or power. The curve for noise sweeps is centered about the average noise power and the one for noise plus signal sweeps is centered to the right of the other by the average signal power. These normalized Gaussian curves have a width which is proportional to  $1/\sqrt{n}$ . ( $n$  = number of sweeps). For a given overlap between them the signal power will, therefore, be proportional to  $1/\sqrt{n}$ . This overlap determines the correlation above chance in the threshold experiments, therefore, the signal threshold power.

$$S_{90} = k/\sqrt{n} . \quad (3)$$

The signal threshold power varies as the reciprocal of the square root of the number of sweeps averaged. This law is a good approximation in computing the effect of changes in pulse repetition frequency (PRF), scanning rate, observation time of the signal, etc. For some factors, the integration properties of the presentation system must also be considered.

The foregoing theory has postulated that the observer can tell which position has the highest average deflection or intensity no matter how small the difference between the two positions. The actual observer cannot meet

---

(4) Threshold Signals, Radiation Laboratory Technical Series, McGraw-Hill.  
(In preparation).

this requirement as is shown by the observations that: (1) the experimental thresholds,  $S_{90}$ , are generally several db above the theoretical values, (2) the slope of the experimental "betting curves" (Fig.1) are much steeper than the theoretical, and (3) two observers of noise, only infrequently (above chance) report the same position as the highest. The "ideal" observer would suffer none of these defects. The actual observer has several inherent limitations:

- (1) Limited ability to integrate. (to remember, to average and to forget)
- (2) A limited angular region of maximum attention.
- (3) Limited angular resolution. (acuity)
- (4) Limited "contrast" discernibility.
- (5) Limited ability to average fluctuations.

In view of these limitations the average value at the signal position must be higher than the average value at the noise positions by a certain minimum factor before any difference is noticed. The discussion of the introduction of such a "contrast" or "averaging defect" factor into the theory is given in Appendix A. While this part of the theory is admittedly as yet in a preliminary state, it does show promise of correlating many effects. The introduction of the proper factor displaces the theoretical threshold,  $S_{90}$ , to about the right experimental absolute value and at the same time gives the theoretical betting curves almost exactly the same slope as the experimental ones.

D. Signal Power, S, Measured Relative to Receiver Noise Power, N.

It is the ratio of the signal power to the noise power in the i-f amplifier which largely determines the signal visibility. In plotting the theoretical or the experimental signal threshold power as a function of various systems parameters the value of signal power, S, is given relative to receiver noise power in the i-f amplifier. (Usually the bandwidth of the i-f amplifier is the reciprocal of the pulse length. The noise power for this is written  $N_1$ ). Once the overall noise figure of any receiver is known the absolute power in watts can easily be calculated for any of the conditions described in this report. Besides being in a highly usable form, one other advantage of this reference level (noise) is its greater accuracy. At present there is greater uncertainty in the measurement of noise figures in many frequency regions than there is in measuring the signal to noise power ratio.

E. Scaling.

From the foregoing it is clear that the signal threshold power,  $S_{90}$ , depends on many parameters (Section B).

$$S_{90} = f(B, b, \tau, s, J, g, T, \text{PRF, scan, focus, spot intensity, etc.})$$

B = i-f bandwidth, Mc/sec.

b = video bandwidth, Mc/sec.

$\tau$  = pulse length,  $\mu\text{sec}$ .

s = sweep speed, mm/ $\mu\text{sec}$ .

J = jamming or interference power.

g = receiver gain.

T = time signal is observed.

PRF = pulse repetition frequency/sec.

There is every reason, theoretical and experimental, to believe that the conditions for discernibility are not changed if the following parameters

are all changed by a factor as indicated since the geometrical pattern presented to the observer is essentially unaltered.

$$\frac{S}{a}, \tau_a, \frac{B}{a}, \frac{b}{a}, \frac{s}{a}, \frac{N}{a}, \frac{J}{a}, \frac{ga}{a}$$

or invariant with

$$S_{90}, \tau, b\tau, s\tau, N\tau, J\tau, \frac{g}{\tau}$$

In the above scaling with change in pulse length, the following parameters should be kept unchanged for the above reasoning to apply strictly: PRF, scan rate, focus, spot intensity, etc. Our results in regard to scaling confirm the British observations on this subject<sup>(5)</sup>, show that the observed relative signal threshold follows the predicted changes to an accuracy well within the probable experimental errors.

### III. EXPERIMENTAL PROCEDURE

#### A. Apparatus.

1. Block Diagram. The apparatus used in the A-scope measurements is shown schematically in the block diagrams of Fig. 3. The names of the components are given as well as the parameters whose values are determined by the corresponding components.

2. Pertinent Characteristics of Components. In Table I a summary is given of the possible settings of each parameter and the component in which the adjustment is made.

a. Azimuth selector. Although designed primarily to turn the signal on at the desired azimuth for use in FPI experiments, this component was also useful in A-scope experiments in that it provides warning bells which tell the observer when to prepare to look for the signal and when the signal is actually on. In the early A-scope experiments these functions were performed by the operator who simply said "Ready",

(5) ADRC Research Report 31, December, 1943

TABLE I. Adjustable Parameters of the Experimental System.

Component where adjustment is made	Parameter	Available range of variation	Values most often used.
Azimuth selector	T, attention interval	0.5 to 60* sec.	T
Mechanical timing switch	Sweep triggering time	1/128 to 6 sec 100 steps	T
Random range selector	Signal positions Number Spread	1 to 50* 1 to 50 mm	
Frequency divider	PRF	3200 to 12.5/sec. (1 step)	
	SRF	3200 or PRF	PRF
Pulse former	T, signal presentation time T, pulse length	0.014 to 15	0.06 and 3.5 sec. 1 usec.
Signal Attenuator	S, signal power at 2nd detector	50 db	
CW attenuator	Sc-w, CW power at 2nd detector	50 db	
Receiver			
	B, intermediate frequency bandwidth	0.2 to 11 Mc/sec	1.2 mc/sec (opt. for 1 usec)
	b, video bandwidth	10 to 0.01 Mc/sec	10 Mc/sec
	Limit level	3 v to 15 v*	no limiting
A-scope	s, sweep rate	10 to 0.055 mm/usec	Fast: 1.7 mm/usec. Slow: 1/20 mm/usec.
	Focus: (spot size)		
	Horizontal	1/20 to 3 mm*	1/20 mm
	Vertical	1/20 to 3 mm*	1/2 mm
	Average noise deflection	0 to 40 mm*	4 mm
	Trace intensity	24 db*	Single trace easily visible
	Type of screen	P-1 and P-7	P-1

\* Continuously variable

"On", and "Off" at the appropriate times. In the azimuth selector a warning bell is automatically sounded one second before the signal is turned on and also at the exact time the signal is presented.

b. Random range selector. In this component the range of the signal was adjusted either manually by turning a potentiometer or automatically by a device which makes a random choice of one of six pre-set potentiometers. Two types of automatic mechanical random selectors have been used.

c. Frequency divider. This component provides triggers for the signal pulse and A-scope sweep. There were nine values of pulse repetition frequency, PRF, ranging from 3200 to 12.5 per second by factors of two. The sweep repetition frequency, SRF, was either equal to the PRF or it was 3200 per second. A coincidence between the master triggers and the output triggers provides for jitter-free operation.

d. Pulse former. The pulse length,  $\tau$ , and presentation time,  $T$ , were established in this component. In addition, it delays the pulse to the range position selected by the random selector.

Phasing was accomplished in a 6SN7 multivibrator, the length of the gate being determined by the R-C time constant from the plate of the first half of the tube to the grid of the second half. R was equal to the resistance of one of the six potentiometers in the random range selector plus the resistance of another potentiometer common to all six. The latter was used for coarse adjustment of all six signal positions simultaneously. Two values of C were used. One gives a minimum delay of 2 usec but excessive jitter at maximum range and was, therefore, used only for experiments in which the sweep length was short. The other was used only in experiments

employing a long sweep since it gives a minimum delay of 80 usec.

The signal presentation time was controlled by another multivibrator whose operation was similar to that of a phasing multivibrator but with, of course, a much longer time constant. When the gate produced by the multivibrator was "ON" the delayed trigger was passed. When "OFF" the direct trigger was passed. Therefore, the r-f pulse generator was being triggered at all times. This is important because the signal power output of the r-f generator is critically dependent on the duty cycle. For example, a reduction of 4 db in output power was observed when the PRF was increased from 200 to 3200/sec.

The video pulse used on the cavity of the 707B r-f generator comes from a circuit employing two thyratrons coupled to a cathode follower. The r-f pulse so produced was adjustable in length from 20 usec down to 0.2 usec and was free from frequency modulation.

e. R-f generators. The r-f pulse generator and c-w generator were 707B tubes completely enclosed in metal containers having only one joint. Special pains were taken to make this joint electrically leak-proof to prevent any leakage power from invalidating the results. A washer, consisting of a helix of 10 mil piano wire wound on a 1/8" arbor and joined into a ring, was compressed between the two sections of the container. The local oscillator was a reflex klystron whose coupling to the mixer was adjusted to give 0.25 Ma crystal current at all times.

f. Attenuators. The signal power,  $S$ , and c-w power,  $S_{c-w}$ , were read from r-f waveguide-below-cutoff attenuators of two different kinds. In the early work double-loop attenuators were used. Later

these were replaced by attenuators which employ an iris to produce a pure  $H_1$  mode <sup>(6)</sup>. This type of attenuator was much more accurate than the earlier type. However, the method used in power measurement tends to cancel out any errors in the linearity of attenuators.

The attenuators were isolated from each other and from the r-f generators by sufficient lossy line (at least 10 db per cable) to prevent interactions.

g. Crystal mixer. The mixer used in these experiments was similar to MEW mixers. It was coupled directly to the receiver without intervening cable.

h. Receiver. The receiver used was one designed especially for the purpose, having a choice of 5 values of i-f bandwidth,  $B$ , and 4 values of video bandwidth,  $b$ . The interstage couplings were double tuned and transitional coupled (flat-flat) with narrowing produced in only one such double-tuned stage <sup>(7)</sup>.

A diode second detector (6H6) followed the i-f stages. Its plate voltage,  $E_2$ , was used as a measure of the output of the receiver in measuring S/N and in experiments involving changes in receiver gain. The response of the second detector was practically linear except for very low voltages.

A video bandwidth of 10 Mc/sec, obtained by shunt peaking in each stage, was normally used. Three other values of  $b$  were obtainable. A bandwidth

---

(6) See RL Report 404, S. G. Sydoniak, September 27, 1943. Model V attenuators whose calibrations are given in this report were used in later experiments. Early experiments were done with Model K attenuators.

---

(7) In the widest band case the results were corrected for the difference between singly narrowed and multiply narrowed noise bandwidth.

of 0.5 Mc/sec was obtained by shunt peaking, using 30K and 5 mh in series from the plate of the first video stage to F 4. For narrower video bandwidths series peaking was used by placing R and L in series from the plate of the first stage to the coupling condenser of the second and C from the latter point to ground. The values of R, L, C, and, therefore, of b were the following:

R (ohms)	L (mh)	C (uf)	b (Mc/sec)
20,000	25	0.0001	100
5,000	35	0.003	10

The maximum output amplitude of the video amplifier, called the limit level, was very high in the receiver described above so that the noise was practically never limited (i.e., the amplification was linear). However, in some A-scope experiments limiting was purposely introduced to determine the effect on the threshold <sup>(8)</sup>. In these experiments MEW receivers were used. Their limit levels were made adjustable by controlling the screen voltage of the 6AC7 tube in which limiting takes place. The limit level at the output of the receivers could thus be adjusted from 3 volts to 15 volts.

1. A-scopes. The usual controls present on all A-scopes were available in the two scopes used in these experiments. In addition it was possible to increase the accelerating voltage of the persistent tube (P-7) in order to get adequate intensity when the sweep speed was very fast.

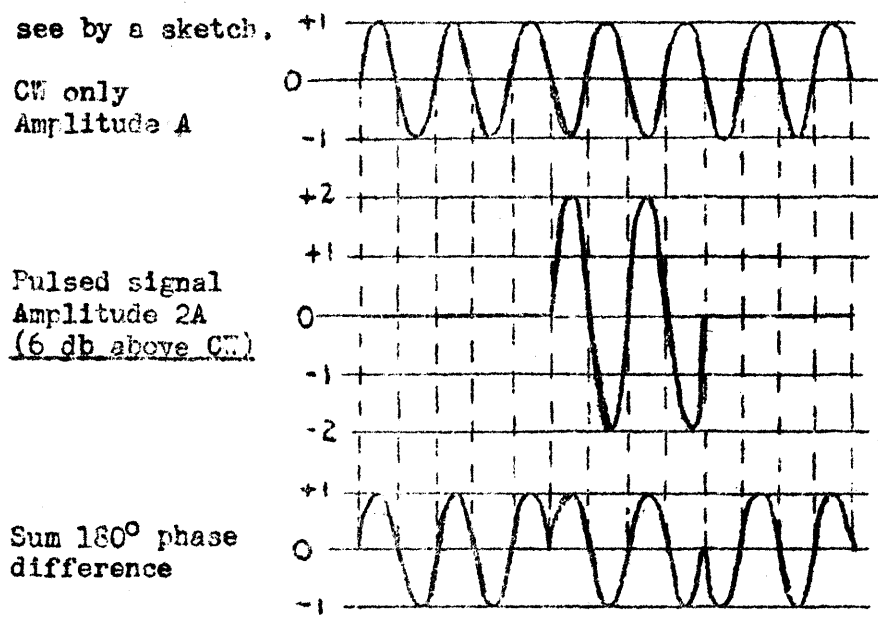
## B. Techniques.

1. Lawson's method of measuring pulsed signal power compared to noise power involves two steps (1) the pulse signal is compared in amplitude to a c-w source at the same frequency. (2) The c-w source is then compared to the noise power in the receiver.

---

(8) NRLFS Report, S. G. Sydorak, December 31, 1945

(a) The comparison of pulsed signal power to c-w power is made by observing the beats between them on an A-scope. The bandwidths should be at least wide enough to give an appreciable flat region on the top of the pulse ( $BT \geq 2$ ) and the gain low so that little noise is showing. Fluctuations or beats in the observed signal amplitude are due to the random phase between the pulse signal and the CW. The relative amplitude is adjusted so that the minimum beat height is just even with the base line. Under these conditions the pulsed signal will be  $180^\circ$  out of the phase and 6 db greater or twice the amplitude of the CW. This may perhaps be made easier to



(Note uniform envelope with phase reversal at beginning and end of the pulse. These reversals of phase necessitate the wide band circuits so that the steady values may be compared independent of the transients introduced at the beginning and at the end of the pulse.) For other phase differences other amplitude of signal will be observed, but these

are of no importance in the measurement; consequently, the amplification may be arbitrarily non-linear without effecting this measurement.

(b) The comparison of c-w power  $S_{c-w}$  and the noise power  $N$  in the desired receiver band was made by means of a voltmeter connected to the output of the linear second detector. The average voltage output of a linear detector due to noise was increased by a factor of 1.45 by the addition of c-w power equal to noise power.<sup>(9)</sup>

Summary of Measurement Procedure:

	Pulse Power	C-W	Noise	Bandwidth	Instrument
(a)	_____			wide	
	↓				
	6 db			$BT \approx 2$	A-scope
	↓	_____			
	↑			as used	meter
	x db				1 to 1.45
(b)	↓	_____	0 db	_____	meter deflection with linear detector

Pulse signal attenuator reading during measurement (a) was  $(6 \pm x)$  db above pulse power equal to noise power.

2. Procedure Followed in Measuring the Signal Threshold; the Six-Position Experiment.

a. Observation of scopes. The experimental results reported in Sec. IV were nearly all for a "six-position experiment". A signal was presented for a time  $T$  at any one of six marked and numbered positions in range on the face of the A-scope or P.I. The signal position was chosen at random but the exact instant at which the signal was turned on was indicated by sounding a bell. A bell was also sounded one second earlier, as a warning to the observer to be ready.

After each presentation of the signal, the observer was required

---

(9) This factor would be  $\sqrt{2}$  except for the difference between the average voltage and the rms voltage.

to name one of the six positions by number as the position having the highest average deflection or intensity and, therefore, most likely to be the signal position. Ten or twenty such observations, made with the same level of signal power and the same value of T, are used to compute the correlation above chance of each signal power level required to obtain the betting curve.

In the A-scope data the average number of observations made by one observer for one betting curve was of the order of 100, but may range from 50 to 200, depending on the accuracy desired and the apparent consistency of the data.

Before beginning observations and particularly before the first group for a given betting curve the observers were allowed a few practice observations. Usually two or three observations were sufficient, but the observer was allowed as many practice observations as he felt he needed to focus his attention and to become familiar with the appearance of a signal of low discernibility.

As an aid in recognizing insufficient practice the experimental points have been numbered in chronological order. If the earlier points are far to the right of all the other points they are given little weight when drawing the betting curve.

b. Conversion of data to correlation scores. The proportion of lucky guesses in a six-position experiment can be easily estimated on the basis that when there was no signal present at all an observer required to name one of the six numbers will make only five misses in six observations, on the average. That is, for every 5 recorded misses he has made one lucky correct guess. The correlation score, p, in per cent, was,

therefore:

$$p = \left( 1 - \frac{6m}{5n_{\text{MAX}}} \right) 100$$

where  $n_{\max}$  was the total number of observations in the group in which  $n$  misses were made. For experiments in which there are other than six possible signal positions the correlation score can be calculated in a similar manner.

c. Drawing the betting curve. From the table of correlation scores the betting curve,  $p$  vs  $S/N$ , was plotted using a linear scale for  $p$  and a logarithmic (db) scale for  $S/N$ . Of course, points having either zero or 100% correlation are given no weight in drawing the straight line through the points.

Examination of a large number of typical A-scope data has shown that characteristically the points will cluster about a straight line such that its 50 per cent and 90 per cent points are 1.6 to 2.2 db apart for all but a few of the most extreme choices of system parameters.

d. Reduction to  $S_{90}$  and  $S_z$ . The signal threshold,  $S_{90}/N$ , was arbitrarily taken to be the abscissa of the betting curve at  $p = 90$ . The signal twilight zone,  $S_z (=S_{90}/S_{50})$ , was then obtained from  $S_{90}/N$  and the abscissa at  $p = 50$ . The signal threshold number and twilight zone number were sufficient to describe the characteristics of the threshold results.

### 3. Factors influencing the accuracy of Signal Threshold Measurements.

a. Apparatus Instabilities and inadequate monitoring have made many experiments reported previously by other laboratories of questionable value. Most of the results and trends measured may be correct but one or two completely misleading results and conclusions tend to nullify all that was done. In the experiments reported here, the method of

measuring the signal power relative to noise is simple and tends to minimize errors. Such monitoring measurements were made at the beginning and end of each betting curve series and only those data accepted for which a check within about 1 db was obtained.

b. Improvement with Practice. After a short period of practice the signal correlation scores obtained by a given observer were recorded and numbered so that recheck could be made as to possible further improvement. These repeats showed that even after months the threshold measurements were stable to within the normal scatter.

c. Statistical fluctuations. The limited number of observations and the limited number of possible signal positions both give rise to statistical fluctuations of the measured thresholds. It appears from the data, that these fluctuations are the same order as the differences between observers.

d. The inherent skill of the observer. Of the nine observers, who participated in the measurements, no one observer was markedly better or worse than the others. The total spread in their average thresholds would be less than 1 db.

e. Fatigue did not appear to be an appreciable factor although ample opportunity was provided for any effect due to it to be made evident.

f. R-f leakage must be eliminated from any threshold measuring apparatus before experiments are begun.

#### IV. EXPERIMENTAL RESULTS ON A-SCOPE

##### A. Statistical Effects.

Included in this group of parameters are those which influence (1) the number of sweeps  $n_s$  of the signal which are averaged in each reading,

(2) the number of sweeps containing only noise that are averaged in with the signal sweep, (3) the number of positions on the tube face or (4) the number of time intervals that must be compared to find the signal position in time, and (5) also the signal presentation time  $T$ , which has to do with the ability of the observer to integrate or average all of the information given him and select it out from larger time intervals. The number of sweeps is, the sweep recurrence frequency multiplied by the presentation time interval.

1. The Pulse Repetition Frequency. The pulse repetition frequency, PRF, was varied from 12.5 per sec to 3200 per sec with all other parameters constant as given in Fig. 4. The results follow the law  $1/\sqrt{n}$  mentioned in Section II over most of the range but begin to show some deviation when the signal threshold is attributable to the decreasing contrast between the signal and the noise positions and the limited contrast discernibility of the observer. The spread of threshold measurements for different observers is seen to be small. Results for three i-f bandwidths are given. Signal presentation time,  $T$ , was 3 sec.

2. Signal Presentation Time. The number of signal sweeps  $n$  is the product of the PRF and the signal presentation time  $T$ . The latter was varied in the experiments of Fig. 5. In the region of signal time between 1/10 and 2 sec the thresholds,  $S_{90}$ , are seen to follow the  $1/\sqrt{n}$  law fairly well, but outside of this region deviations become appreciable.

In the region of very short presentation time this deviation is attributable to the inability of the observer to integrate only during the signal presentation interval. The same observer characteristics which cause flicker to disappear somewhere between 25 and 100 cycles/sec also cause the observer to integrate some of the noise sweeps immediately preceding or following the

signal presentation interval.

At long signal presentation times, the deviation from the  $1/\sqrt{n}$  law is attributable to the observer's inability to remember all of the data given him. Finally, he will probably forget data at the same rate it is presented to him and the threshold curves will level off to a limit. The experimental curves can be fit very well by assuming a minimum integration time, corresponding to the first effect and a maximum integration time of about six seconds corresponding to the second effect.

At the long signal presentation times, difference between the thresholds for F1 and F7 A-scope, screens are seen to be of the order of one or two db but the difference is essentially lost at short times.

3. Extra Noise Sweeps. In the above experiments on repetition frequency and observation time the observer was always informed as to when the signal was being presented. A study was made of the effect of increasing the uncertainty as to the particular sweeps and exact range positions containing the signal. In the first experiment of this type, extra sweeps containing only noise were introduced between sweeps containing the signal and noise by triggering the sweep at a constant rate of 3200/sec and using different pulse repetition frequencies. The results are shown in Fig. 6.

As long as  $S_{90}/N < 43$  db it is inversely proportional to the number of signal sweeps in agreement with the theoretical results for an Ideal Observer. When the signal threshold power is greater than this, however, there is a deviation from the predicted dependence. This is believed to occur because the actual observer no longer uses average power as a criterion, but finds it much better to examine only the few deflections of very high amplitude. This is one of a number of instances which have been noted in which superposition of signal and noise traces is not equivalent to presentation of the average power as is assumed in effect in the theory.

At low  $S_{90}/N$ , the P7 screen was better than the P1 because it helps to average out the light intensity at each amplitude. At high  $S/N$  the P7 screen was worse because it cuts down relatively on the instantaneous intensity of the few deflections of high amplitude which are most useful.

In a similar way, if the PRF is held constant at 200/sec and noise sweeps are added as shown in Fig. 7 by triggering the A-scope more often, the signal threshold,  $S_{90}$ , rises at the theoretical rate, proportional to the square root of the total number of sweeps.

When the signal threshold power,  $S_{90}$  is comparable to i-f noise power, the signal threshold power is proportional to the square root of the total number of sweeps, divided by the number of sweeps containing the signal.

$$S_{90} = k \frac{\sqrt{n_{\text{total}}}}{n_{\text{signal}}} \quad (4)$$

4. Number of Range Positions. If the number of possible signal positions in range is increased, the signal threshold power increases. Fig. 8 gives the results of two experiments in which the possible range positions were changed from two to fifty. The spread of the positions was different in the two experiments. The one started with two positions 1 mm apart; the other, 50 mm apart. The difference is 2 db. (Attention is called to the expanded vertical scale of Fig. 3 compared to other figures). The difference between these experiments is, due to the better attention or acuity possible over the smaller angular cone compared to the larger cone.

5. Signals Random in Time. Similar to the increase of the number of possible range positions, the number of possible positions in time may be increased by having the signal occur at random time, (but still of definite duration known to the observer) in a larger time interval. From a theoretical standpoint, the problem was the same. In the experiment of Fig. 9, the

attention interval was increased from 1/10 sec (equal to the signal presentation time) to 20 sec, a factor of 200; from 6 range positions, to  $6 \times 200 = 1200$  range-time positions.

## B. Geometrical Parameters.

Included somewhat arbitrarily in this group of parameters were those that have an influence on the geometrical appearance of the trace on the A-scope.

1. I-f Bandwidth x pulse length,  $B\tau$ . As shown in Fig. 10 the i-f bandwidth x pulse length has a broad optimum at  $B\tau = 1.2$ .

At high values of  $B\tau$  ( $>10$ ) the signal threshold appears to increase linearly with  $B\tau$ . This corresponds to the increase in noise power in the pass-band without a corresponding increase in signal since most of the signal power is included in the pass-band when  $B\tau = 1$ .

For low values of  $B\tau$ , ( $<0.1$ ), i-f bandwidth too narrow, the signal amplitude is approximately proportional to the bandwidth, with the noise power still proportional to the bandwidth. This results in the inverse linear relationship of the signal threshold  $S_{00}$  that exists in this region.

Although not critical an i-f bandwidth corresponding to a  $B\tau$  of 2 appears to be a reasonable compromise between rate of recovery from overload and increase in threshold.

2. Video Bandwidth x pulse length,  $b\tau$ . Although the data presented in Fig. 11 are rather meager, they show that the signal threshold is relatively independent of video bandwidth, if  $b$  is greater than one-half the i-f bandwidth. If a slow sweep is used, still further narrowing of the video is possible before additional rise in signal threshold is observed.

However, recovery from overload, especially the influence of jamming or interference makes a video bandwidth x pulse length of not less than 1,

perhaps 2 seem very desirable. (10)

### 3. Video Coupling - Rejection of Low Frequencies by R-C Differentiation.

Experiments using 1  $\mu$ sec pulses were performed in which the i-f bandwidth was optimum 1.1 mc/sec and the video 3-db down frequency on the high side of the pass band was 10 mc/sec. The coupling time constant, which would effectively determine the 3-db frequency on the low side of the video pass band, was made successively smaller until the time constant was 1/10  $\mu$ sec. Even under this extreme differentiation less than 1 db rise in the signal threshold was recorded. Additional video gain was required under these conditions. The absence of influence was attributable to the fact that the noise is also differentiated equally with the signal.

4. Sweep rate, s, mm/ $\mu$ sec multiplied by pulse length  $\tau$ / $\mu$ sec. The results of both PPI and A-scope experiments are given in Fig. 12. A broad optimum was observed when the signal length,  $s\tau$ , on the PPI or A-scope was approximately 1 mm. For values shorter than this, as most often used in radar presentation, the signal threshold rises significantly.

The data of Fig. 12 were taken using several different i-f bandwidths and pulse lengths. In every case the observed threshold confirmed the scaling principles discussed above in Section II.

5. Focus. As shown in Fig. 13 defocusing perpendicular to the direction of the sweep was found to have negligible effect on the threshold as long as the spot was not greater than the noise amplitude. Defocusing in the direction of the sweep also had little effect on the threshold even on slow sweeps, until the spot size was 1 mm or greater. This fact and the preceding observation of an optimum pulse length on the presentation of 1 mm imply that the observer makes little use of fluctuations appearing in less than 1 mm. Assuming

---

(10) Refer to PL Report 220 by J. M. Alfred and A. L. Gardner.

an "observer video bandwidth" dependent on sweep speed, Uhlenbeck has satisfactorily correlated the video bandwidth, sweep rate and focus data.

6. Receiver (i-f) Gain. Figure 14 shows the dependence of the signal threshold,  $S_{90}$ , on receiver gain. Almost no increase in  $S_{90}$  is observed until nearly all of the noise has disappeared from the trace; after that the trace height is the controlling factor. A constant signal amplitude is required; therefore,  $S_{90}$  varies inversely as the receiver gain as would be expected.

7. Sweep Direction. Because of rumors of a large dependence of signal threshold on sweep direction, a few observations were made on a vertical A-scope sweep. In spite of few observations to practice on, the vertical sweep threshold measurements were within 1 db of the much-practiced horizontal-sweep thresholds.

#### C. Contrast Effects.

1. Trace Intensity. The contrast in light intensities between the A-scope trace and the surrounding region was examined briefly and found to be completely unimportant under the conditions examined. The results are shown in Fig. 15. In this experiment the trace intensity was varied from the maximum obtainable, much brighter than used in practice, to the point, some 60 db lower, at which the trace was barely visible. A total change in the threshold of only 3 db was observed. Of this, 2 db occurred at the lower end. The threshold was constant, within experimental error, for the first 40 db of decreasing intensity. In this experiment the ambient light was kept at a minimum. For the sake of completeness it would be desirable to keep the trace intensity constant and progressively increase the ambient light, but this experiment was not done.

2. Evidence of contrast effects. Imperfections in the observer's ability to tell which position has the highest average intensity or deflection lead to at least three differences between the experimental results and the theoretical thresholds calculated for the "ideal" observer, without these imperfections.

- (1) The experimental thresholds,  $S_{90}$ , were generally several db above the ideal theoretical values (calculated by Uhlenbeck and Fang) as seen in Fig. 16. The data are averages over a large number of experiments.
- (2) The slope of the betting curves was greater for the experimental curves than for the theoretical Ideal Observer, as shown in Fig. 17, where the width of the "twilight zone" was presented, that is, the ratio of  $S_{90}$  to  $S_{50}$ , the theoretical value being 2.8 db.
- (3) Two observers of noise if "ideal" would always report the same position as the highest. Actual observers show little correlation. In Fig. 18 the correlation of coincidence misses for two observers is given; that is, if the two observers named a noise (no signal) position as being the highest, Fig. 18 gives the probability of their naming the same noise position.

In each of these cases the deviation of the actual observer from the theoretical or ideal observer increases as the number of pulses to be integrated increases.

The observed peculiarities in the shape and displacement of betting curves can be approximately reproduced theoretically as shown in Fig. 19 on the assumption that the observer exhibits an "averaging defect",  $\delta$ , such that

$$\delta = k/\sqrt{n}$$

In this expression,  $k$  is a constant, and  $n$  the number of signal pulses observed.

The averaging defect,  $\delta$ , is defined as the minimum discernible fractional difference in the average intensities at two points on the radar screen. The theoretical method for deriving a betting curve when  $\delta \neq 0$  is described in Appendix A. Several betting curves calculated by this method for various values of  $n$  and  $\delta$  are shown in Fig. 19. There is a progressive steepening and upward displacement of the betting curves as  $\delta$  increases. For a given displacement of the betting curve,  $\delta$  is less at high  $n$  than at low  $n$ . This is in the proper direction to be qualitatively in agreement with experiment.

The approximate value of  $k$  can be determined from Figs. 16 and 17 which show the results of an analysis of 24 measured betting curves taken at  $T = 3$  sec and  $n = 40, 600, \text{ and } 10,000$ , and theoretical results taken from Fig. 19c. It should be pointed out that the theoretical results shown here were not read directly from the curves of Fig. 19c but from straight lines drawn to approximate these curves in the range from 20% to 90%. This was done because the experimental betting curves were drawn in a similar manner; i.e., by drawing a straight line through the distribution of experimental points.

Of the two values of  $k$  which were chosen when calculating the betting curves,  $k = 5.6$  best fits the experimental data of Fig. 16. Unfortunately a complete set of calculations for this value of  $k$  and other values of  $n$  was not made but presumably its shape would be somewhat the same as the one shown for  $k = 2.8$  and a reasonably good fit for low values of  $n$  with some deviation at higher values would exist. Apparently the assumed function takes care of an averaging defect but not a limited contrast discernibility. If  $k$ , in the assumed function  $\delta = k/\sqrt{n}$ , is assumed to be 2.8, then the observed and calculated twilight zones vary in the same way, although the calculated curve is somewhat higher than the experimental points. On the other hand,

$k = 5.6$  gives a point which is too low, indicating that an intermediate value would give the best fit.

5. Law of the Receiver. Except when limiting, the law of the receiver is believed to have little effect on the signal threshold power for A-scope since the observer can weight the deflections according to any law compatible with his limitations. Information may be lost if severe limiting takes place and the signal threshold power,  $S_{90}$ , may be much higher. (11)

#### V. SIGNAL THRESHOLD MEASUREMENTS ON PPI

Using the same techniques as for the A-scope, measurements were made of the signal threshold power  $S_{90}$  on the PPI. Parameters investigated were PRF, signal presentation time, i-f bandwidth times pulse length, random signal azimuths, overlap from scan to scan, dependence on angular arc. The dependence on pulse length on the screen is given along with the A-scope data on the same subject, Fig. 12.

##### A. PRF

Laboratory experiments on a PPI scope made to determine the effects of the variation of the pulse repetition frequency of the radar system on the signal threshold power indicated approximately the same results, within the limits of experimental error, as on the A-scope for the region investigated. The results appear in the graph in Fig. 20. It is quite possible that the results might be different on a particular operating radar system since the effect of video limiting on threshold power is quite marked. (11)

##### B. Signal Presentation Time, T.

PPI tests were also made to determine the effect of the variation of the signal presentation time,  $T$ , on the signal threshold power. In these tests,  $T$ , was variable from 0.004 to 7.5 sec, PRF was 300 cycles/sec, a signal was turned on at  $90^\circ$  azimuth with a scanning speed of 7.5 rpm.

The results for two observers are shown in Fig. 21.

As in the A-scope experiments, and in agreement with the theory, a square-root relationship was found to hold over a wide range of T; from  $T = 0.01$  to 1 sec,  $S_{90}/N = k/\sqrt{T}$ . This range of T is equivalent, at the scanning rate used, to a range in antenna beam angle from  $0.5^\circ$  to  $45^\circ$ . At the average signal position (average target range) the length of the arc of signals ranged from 0.3 mm to 25 mm.

At  $T = 0.004$  there is an average of only 3.2 pulses per scan and the deviation from the square root dependence is 5 db (poorer discernibility). At  $T = 7.5$  sec the threshold is again above the square root curve (2 to 3 db higher). These deviations are comparable to those obtained for A-scope experiments. The deviation at low T is due, at least in part, to the small geometrical dimensions of the signal and the resulting inability of the observer to disregard extra noise adjacent to the signal position. At high T, the extra loss is probably due to the inability of the observer to estimate the average intensity over a very long arc.

C. The Effect of the Variation of the Product of I-f Bandwidth and Pulse Length on the Signal Threshold Power.

PPI tests were made to determine the effect of variation of the product of i-f bandwidth and pulse length on the signal threshold power. The results which are shown in Fig. 22, are very similar to those on the A-scope. In this experiment, there were two observers. The PRF was 391 cps, The signal presentation time, T, was 1/16 seconds. The pulse length  $\tau$  was 1.0  $\mu$ sec, and the sweep speed was 0.63 mm/ $\mu$ sec.

D. Random Possible Signal Azimuths.

In the previous experiment the signal was always at a marked azimuth, ( $90^\circ$ ) from the "top" end of the screen) so that the observer knew where to focus his attention. In this experiment, the signal azimuth was chosen at

random so that the observer had to examine the entire face of the tube for the signal. Two such experiments were performed. At  $T = 0.004$  sec and 7.5 rpm, the loss due to increasing the range of signal azimuths to  $360^\circ$  was 2.4 db. At  $T = 0.25$  sec and 2 rpm the loss was 1.8 db.

#### E. Overlap.

Because of the persistence of a P-7 screen, a signal which remains at the same position from scan-to-scan can be seen more readily on one of the later scans than on the first scan. That is, when a signal overlaps on successive scans the effective signal presentation time increases.

Although overlap was not purposely provided in the first PPI experiments, the random choice of one of six signal positions resulted in the occurrence of an appreciable number of repeats. In analyzing these repeats, it was found that the choice of an observer, after one overlap, was better than the choice with no overlap. Of 192 repeats, in which the first or the second choice of an observer was correct but not both, the probability was 42% that the first was right and 58% that the second was right. Assuming a typical betting curve for which the correlation score rises 20% per db rise in signal power, the improvement due to one repeat at the same signal position is, therefore, 0.8 db. Theoretically the maximum possible improvement would be 1.5 db, the improvement due to doubling the signal presentation time.

Further work in determining the effect of signal overlap on signal threshold power was done on the PPI of an actual radar system using both a target airplane and a signal generator as a source of signal. When the airplane was used, the percent of signal overlap depended on both the speed of the airplane, and the scanning speed of the antenna. Since the speed of the airplane could not be varied over a wide enough range to vary the percent overlap appreciably for any given scanning speed, no conclusive results

could be obtained. However, the signal generator was designed to produce a signal variable over 60 db in intensity and movable in a range at a variable speed corresponding to an air speed of 40 miles per hour to 600 miles per hour. The results are shown in Figs. 23 and 24. The system used had an antenna pattern  $1.5^\circ$  wide in azimuth, the pulse length was 1  $\mu$ sec, and the PRF was 400 cycles/sec. The airplane used was a Curtiss Wright monoplane with a cruising speed of approximately 100 miles/hour.

#### F. Dependence on Angular Arc.

The signal appearing on the PPI of a radar system having a very broad antenna pattern will show as an arc, while that from a system with a very narrow antenna pattern will appear as a spot. Since the shape of the two signals is so different it was felt desirable to find how the signal threshold power depended on the angular arc of the signal.

In this experiment, the time, T, that the signal was presented, was kept constant at  $1/4$  second, the scanning speed was varied from 0.5 rpm to 120 rpm, and the signal was turned on each time at an azimuth of  $90^\circ$ . The PRF used was 300 cps. One observer did the experiment.

From 2 to 30 rpm the threshold did not change appreciably (less than 1 db spread in the points). At 120 rpm, the loss was about 2 db. In other words, from antenna beam angles of less than  $0.5^\circ$  up to  $45^\circ$  the threshold was essentially constant, but when the signal was spread out over  $360^\circ$  a 2 db loss was obtained. The results are shown in Fig. 25.

#### G. Equation for Estimating Scanning Loss

One implies from the deviation of Fig. 5 from the theoretical dependence of  $1/\sqrt{n}$  and also especially from the independence of the aircraft signal curve of Fig. 24 above 10 rpm, that the information in an interval of from 6 to 10 sec is all that is useful to the observer. In other words, the observer

see essentially as small a signal in 6 to 10 sec as he could if the system "searchlighted" on the target for a much longer period. Therefore, the signal threshold power for 8 sec<sup>(12)</sup> on target is used as the "searchlighting" value from which the increase in signal power required for detection under scanning conditions (scanning loss) is computed.

From the best information now available "good" radar operators require a signal about 3 or 4 db above  $S_{90}$  of these experiments. This minimum useful signal power,  $P_{min}$ , varies in the same way as  $S_{90}$ . To stress this difference and to use a notation nearer that of other discussions of maximum range radar systems,  $P_{min}$  will be used in this section.

If 8 sec, the information of Figs. 4, 5, 6, 7 and 24 can all be correlated quite well with the relationship for  $P_{min}$ .

$$P_{min} = \frac{k \sqrt{n_{total}}}{n_{signal}} \quad (5)$$

$$n_{total} = n_{signal} + n_{noise} \quad (6)$$

Where  $n_{total}$  is the total number of sweeps in a beamwidth,  $n_{signal}$  is the number in which signal power is present and  $n_{noise}$  the number having only noise present at the range being considered.

1. Simple Scans. In this expression  $n_{total} = n_{signal}$  except for complex systems, as those involving scanning in both azimuth and elevation. Equation (5) for simple scans reduces to:

$$P_{min} = \frac{k}{\sqrt{n_{signal}}} \quad (7)$$

With the aid of this equation let us compute the approximate scanning loss for a system having an azimuth beam width,  $H$ , of  $3^\circ$ , scanning in azimuth at  $R$  revolutions per minute ( $R \leq 8 \text{ rpm}$ ). The value of  $sP_{min}$  for searchlighting

---

(12) Any value from 6 to 10 sec could be used within the accuracy of the approximation.

will be given by

$$s^{P_{\min}} = \frac{k}{\sqrt{8 \text{ PRF}}} \quad (8)$$

The angle scanned through in 8 sec is  $\frac{8}{60} \times 360^\circ \times R = 48R$  and the number of signal sweeps is therefore,  $\frac{R}{60} \times 360 \times 8$ .

$$\text{Therefore, } P_{\min} = k \sqrt{\frac{48R}{8 \text{ PRF} \times H}}$$

$$\frac{P_{\min}}{s^{P_{\min}}} = \sqrt{\frac{48R}{H}} \quad \frac{H}{48} < R < 8 \text{ rpm} \quad (9)$$

For  $3^\circ$  beamwidth and 4 rpm the scanning loss is  $\frac{48 \times 4}{3} \approx 8$  or approximately 9 db

All this loss would be gained back by scanning so slow that the beam just moved across the target in 8 sec. ( $3^\circ$  in 8 sec or  $\frac{1}{16}$  rpm). No more could be gained by scanning slower than this.

For the case when  $R > 8$  rpm for essentially stationary targets scan to scan integration of the signal takes place as indicated by Fig. 24. The scanning loss is given by

$$\text{Scanning Loss} = \sqrt{\frac{360}{H}} \quad (10)$$

This law may be expected to apply up to target velocities such that the target moves a distance equivalent to about  $\frac{1}{2}$  of the pulse length from one scan to the next, ( $v < 2.8 R\tau$  and  $R > 8$  with  $v$  in mph,  $R$  in rpm and  $\tau$  in  $\mu\text{sec}$ ).

For target velocities greater than this (order of  $57R\tau > 2.8 R\tau$ ) integration of the noise sweeps, which overlay the signals, from scan to scan compensates for the integration of signals from scan to scan and the threshold would be expected to vary approximately as the square root of the scanning rate for  $R > 8$  rpm as in equation 9.

If the spot has moved of the order of 10 pulse lengths between scans, correlation of two or more positions in such a way as to provide effective integration of their signal information seems extremely unlikely. Therefore,

for very high speed targets ( $V > 57 R/T$  and  $R > 8$ ) the total number of sweeps in a beamwidth in 8 sec will be constant at  $n_{total} = \frac{H \times 8 \text{ PRF}}{360}$  and the number of these sweeps containing the signal will be inversely proportional to  $R$ . Equation 5 applies for the threshold and the scanning loss will be proportional to the scanning rate.

2. Complex Scans. Consider the scanning loss of a system having the following characteristics: vertical beamwidth  $1^\circ$ , horizontal beamwidth  $5^\circ$ , elevation scan  $15^\circ$ , 4 scans/sec., azimuthal scan 3 rpm =  $18^\circ/\text{sec}$  and presentation PPI. The total number of sweeps in a beamwidth,  $n_{total}$  is in 8 sec:

$$n_{total} = \frac{(8 \text{ PRF}) 5}{8 \times 18} = \frac{5}{18} \text{ PRF}$$

For the number of signal sweeps in 8 sec assuming a linear vertical scan:

$$n_{signal} = \frac{1}{15} n_{total} = \frac{1}{54} \text{ PRF}$$

For "searchlighting":  $s n_{total} = s n_{signal} = 8 \text{ PRF}$

Therefore, the scanning loss from equation 5 will be approximately:

$$\begin{aligned} \text{Scanning Loss} &= \frac{P_{min}}{P_{smin}} = \frac{\sqrt{\frac{5}{18} \text{ PRF}}}{\frac{1}{54} \text{ PRF}} \sqrt{8 \text{ PRF}} \\ &= 36 \sqrt{5} \text{ or } 19 \text{ db.} \end{aligned}$$

In general for a complex scan which searches a vertical angle  $B^\circ$  at a high rate and at the same time searches more slowly in azimuth through an angle of  $A^\circ$  in 8 sec., the total number of sweeps ( $n_{total}$ ) in a given beam width  $H^\circ$  on the PPI is inversely proportional to  $A^\circ$ . The number of signal sweeps ( $n_{signal}$ ) is inversely proportional to  $B^\circ$  and directly proportional to the vertical beam width  $V^\circ$ .

The scanning loss for fixed targets for this case from equation 5 is

$$\begin{aligned} \text{Scanning Loss} &= \sqrt{\frac{A}{H}} \frac{B}{V} \\ \text{in db} &= 5 \log \frac{A}{H} + 10 \log \frac{B}{V} \end{aligned}$$

Further losses on high speed targets are to be expected as in the above example of the simple scan and can be estimated in the same way as was done there.

In using these equations one should remember that most of the experiments on which they are based were with signals below  $\pm 10$  db relative to noise in optimum bandwidth. Extrapolation into higher signal to noise regions should be regarded at best as approximations especially in view of such deviations from the laws in these regions as those in Fig. 6. The experimental systems used were linear throughout as nearly as could be achieved. Non-linearities are expected to influence signal threshold especially when the threshold signal is large compared to noise in optimum bandwidth.

## APPENDIX I Theoretical Setting Curves for an Observer with an Averaging Defect

By S. G. Sydorak

### A. Definition of Contrast and Averaging Defect.

Ordinarily minimum discernible contrast is defined as the ratio of light intensities of a just discernible uniformly illuminated patch on a uniformly illuminated background. Unfortunately this ratio minus unity is also sometimes called "contrast" in the literature although it is more correctly called the Fechner fraction. Numbers often used to represent the minimum discernible contrast range from 1.02 to 1.04<sup>(1)</sup>. However, recent experiments have shown<sup>(2)</sup> <sup>(3)</sup> that the correct number is often considerably higher than this and is critically dependent on the area of the patch and on the brightness of the background, especially when this is less than 1 equivalent foot-candle.

When both the patch and the background fluctuate, as in the case for radar signals surrounded by noise, the rms deviation of the fluctuation will be an additional factor in determining the minimum discernible contrast. Due to the fluctuation the observer may experience greater difficulty in recognizing a difference in the average amplitude (or average intensity, in the case of PPI presentation) of a signal compared to that of noise. It would, therefore, be expected that the "minimum discernible contrast" differ for fluctuating signals than for steady illumination.

- 
- (1) D. O. North "An Analysis of the Factors which Determine S/N Discrimination in Pulsed Carrier Systems" R.C.A. Technical Report PTR 6-C uses 1.02 to 1.04 which he obtained from a report by H. E. Kallman "The Gradation of Television Pictures" IRE vol 23, No. 4, pp 170-174, April 1949.
  - (2) R. G. Hopkinson "Visibility Problems Associated with the Skiatron" GEC 8039 (RL No. 3594) finds that under operational conditions a contrast ratio of less than 1.06 is not appreciable. He also notes that the dark adaptation of the observer and the width of the trace are important.
  - (3) J. Fairbairn and R. G. Hopkinson "Visibility of PPI Traces on Cathode Ray Tubes. Traces on Uniform Backgrounds." GEC 8506 (RL No. 4042) July 7, 1944. They have measured minimum discernible contrast ratios ranging from 1.01 for large areas in bright surroundings to upwards of 100 for small areas in dim surroundings.

To avoid confusion with the usual case of steady illumination and because the observers do not wish to limit themselves to speaking of light intensities, it has been useful to introduce a term, analogous to the Fechner fraction, which is called the "averaging defect of an observer of radar signals". The averaging defect for the case of PPI presentation is defined as the minimum discernible fractional increase in the average intensities at two points on the radar screen. Thus if A and B are the intensities averaged over n sweeps at points  $P_A$  and  $P_B$  respectively on a radar screen and A is just noticeably brighter than B, then the averaging defect  $\delta = A + B/B$  where A and B are defined as the average of the squares of the amplitudes at the two range marks. A being just noticeably higher than B. For the case of steady illumination the ratio of A to B is in fact the minimum discernible contrast ratio and  $A/B - 1$  is the Fechner fraction. The Fechner fraction is, therefore, seen to be analogous to the averaging defect as defined above for fluctuating signals on a noisy background.

#### B. Uhlenbeck's Theoretical Relations.

Let  $z$  be the average of the PPI intensity (or the average of the squares of the amplitudes of the A scope trace) on n sweeps at a noise position and  $z'$  be the average intensity at a signal position. Also let  $\bar{z}$  and  $\bar{z}'$  be the grand averages of  $z$  and  $z'$  when the same experiment is repeated an infinite number of times,  $n$  being constant. Then  $\bar{z}$  is the average noise power, called  $2W$ , and  $\bar{z}'$  the average signal power, called  $\beta^2 + 2W$ , the ratio  $\bar{z}'/\bar{z} = (\beta^2 + 2W)/2W$  being the signal to noise power ratio, elsewhere in this report called S/N. For the signal position the probability that  $z'$  will occur in a particular experiment is then given by the relation.

$$P'(z', n) = \frac{1}{\sqrt{2\pi\sigma^2}} e^{-\frac{(z' - \bar{z}')^2}{2\sigma^2}}$$

where  $\sigma^2 = (z' - \bar{z}')^2 = z'^2 - (\bar{z}')^2 = (2W/n)(\beta^2 + W)$ .

For the noise position, the probability that  $z$  will occur is

$$P(\bar{z}, n) = \frac{1}{\sqrt{2\pi} \sigma} e^{-\frac{(z - \bar{z})^2}{2\sigma^2}}$$

where  $\sigma^2 = 4W^2/n$ .

These distribution functions are shown in Fig. A1 to which we shall now refer in explaining the method we used to calculate betting curves for the case of an observer who has an averaging defect  $\delta$ .

C. Betting curve calculations for the two-position experiment.

Suppose in a particular observation, that the average intensity at the signal position is  $z'$ . At the noise position, the intensity can be either noticeably less, in which case the observer will be correct, or noticeably greater, whereupon the observer will be wrong, or in the region between, where the observer is not aware of a difference in intensity and will, therefore, be forced to guess. The two limits of the latter region will be such that  $\frac{z}{z'} = 1 + \delta$  and  $z'/z = 1 + \delta$ .

The condition for which the observer will merely guess at random is, therefore,

$$z'/(1 + \delta) < z < z' (1 + \delta)$$

The probability that the observer will simply guess is, therefore, equal to the area B in the figure and for a two-position experiment his score when this happens will be, on the average, 50%. Whenever  $z < z'/(1 + \delta)$ , and the probability that this will occur is given by area A, the observer will be 100% correct. Therefore, his average score when the signal amplitude is  $z'$  will be

$$s = A + B/2$$

Of course, the signal intensity can have any value and to obtain the total score  $S$  a double integration must be performed according to the following mathematical formula

$$S = \int_0^{\infty} (A + B/2) P(z', z) dz'$$

or, converting to correlation score according to the method of Sec. IIIB, 2b

$$\overline{CS} = 2S-1 = +1 + \int_0^{z'} \frac{e^{-\frac{(z-\bar{z})^2}{2\sigma^2}}}{\sqrt{2\pi\sigma^2}} dz + \int_{\frac{z'}{1+\delta}}^{z'(1+\delta)} \frac{e^{-\frac{(z-\bar{z})^2}{2\sigma^2}}}{\sqrt{2\pi\sigma^2}} dz - \int_0^{\frac{z'}{1+\delta}} \frac{e^{-\frac{(z'-\bar{z}')^2}{2\sigma'^2}}}{\sqrt{2\pi\sigma'^2}} dz'$$

The actual calculation was performed by double numerical integration, taking some 15 intervals in  $z'$ , multiplying the area of each interval by the function  $s$ , and summing up. The function "s" corresponding to each value of  $z'$  is evaluated by a separate numerical integration.

D. Betting curve calculations for the six-position experiment.

The theory of the extension of the above method to the case of a six-position experiment is the following: Suppose, as before, that the signal intensity is in the interval shown at  $z'$  in Fig. A1. The probability that the intensity at all five noise positions will be below  $z'/(1+\delta)$  is equal to  $A^5$ , since the intensity at any position is independent of the intensity at any other position, (the positions being several pulse lengths apart).

Similarly,  $A^4B$  is the probability that a particular noise position, say position No. 1, will fall in region B at the same time that the other four noise positions fall in A. When this event occurs the observer will make a pure guess between position No. 1 and the signal position and the score will be  $A^4B/2$ . But since any of five positions can fall in region B when the others fall in A, the contribution to the total score of such events is  $5 A^4B/2$ .

By a similar line of reasoning the other possible combinations can be derived. Of course, any combination that puts one or more noise positions in region C automatically causes the observer to make a wrong statement. We thus obtain for the net score whenever  $z'$  occurs,

$$s = A^5 + \frac{5}{2} A^4B + \frac{10}{3} A^3B^2 + \frac{5}{2} A^2B^3 + A B^4 + \frac{1}{6} B^5$$

where

$$A = \int_0^{z'(1+\delta)} P(\bar{z}, n) dz \text{ and } B = \int_{z'/(1+\delta)}^{z'(1+\delta)} P(\bar{z}, n) dz$$

Integrating over  $z'$  we have for the total score

$$S \int_0^{\infty} s P'(\bar{z}', n) dz'$$

or, converting to correlation score we have, for the six-position experiment

$$\overline{CS} = \frac{6}{5} S - \frac{1}{5} = \frac{6}{5} \int_0^{\infty} s P'(\bar{z}', n) dz' - \frac{1}{5}$$

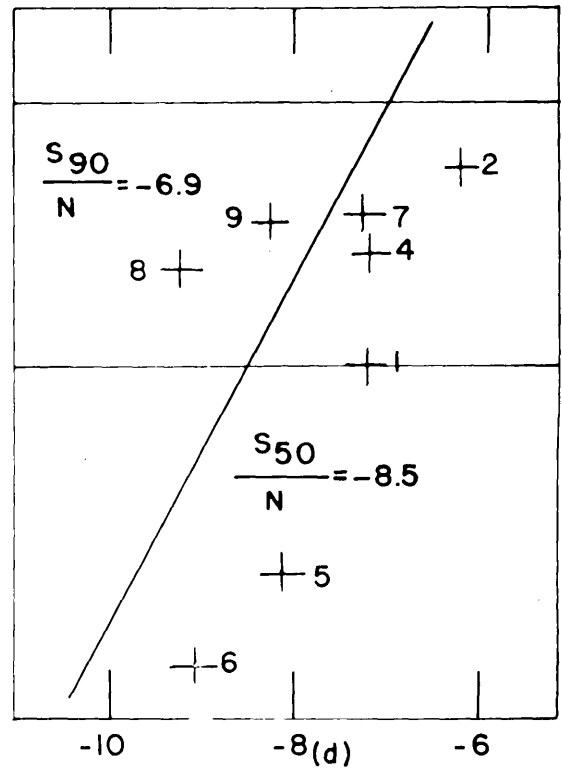
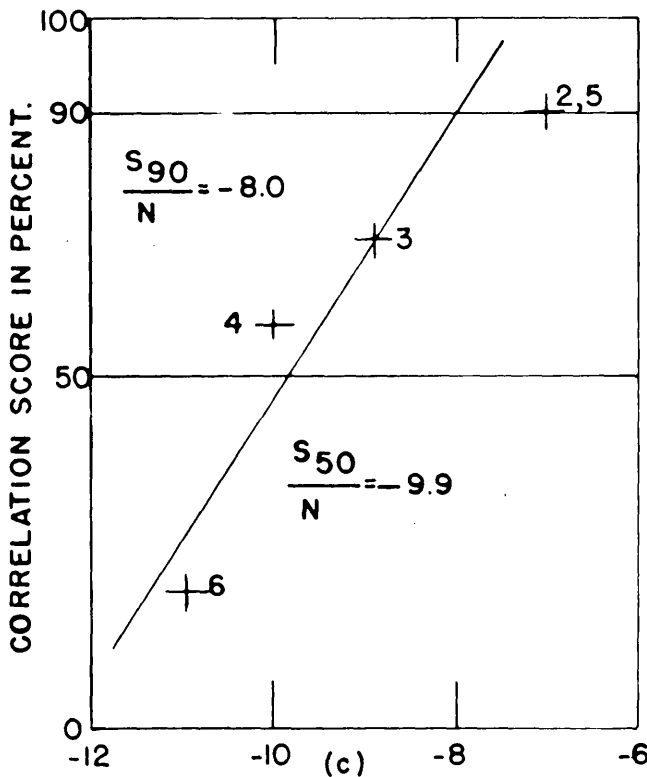
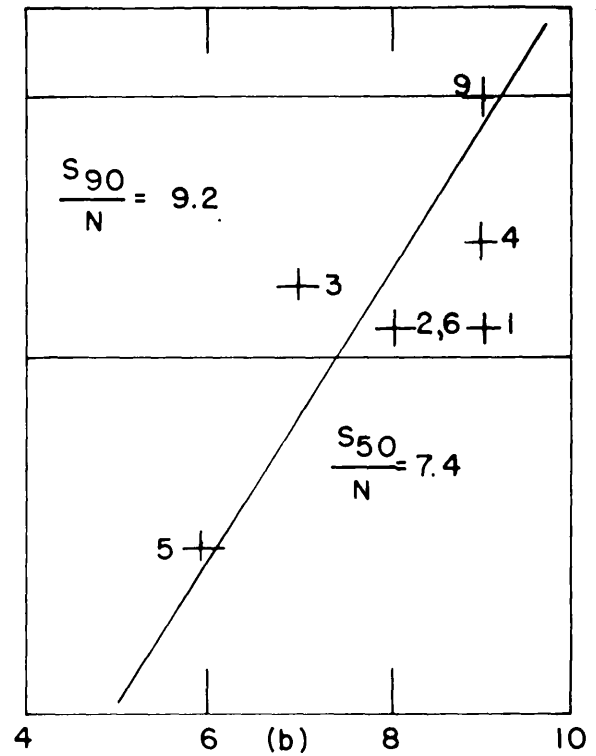
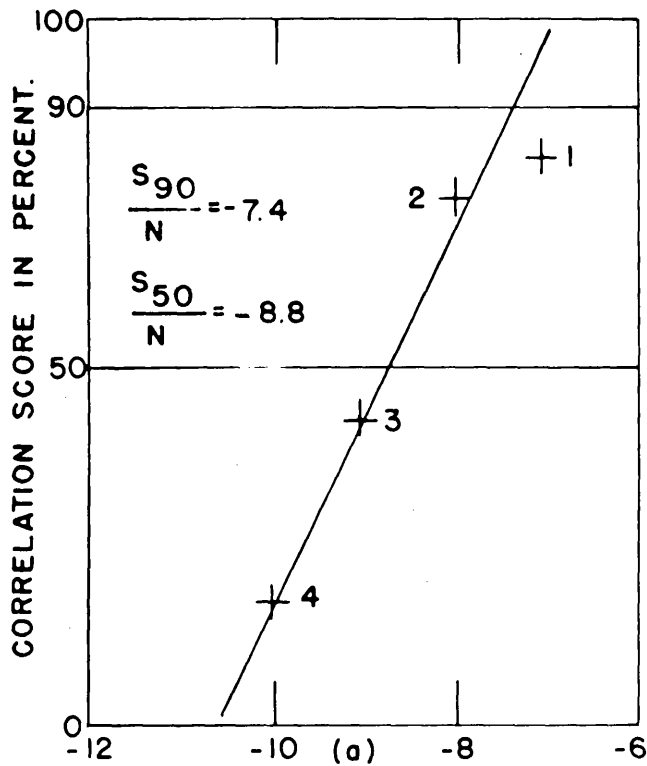
By the same process of double numerical integration used for the two-position experiment the betting curve can be obtained for any signal to noise ratio  $\bar{z}'/\bar{z}$  and any value of  $n$ . To eliminate the labor involved in repeated calculations of the function  $P'(\bar{z}', n)$  for different values of  $z'$  a nomograph was constructed of the single curve.

$$\int_{-\infty}^{z-\bar{z}} e^{-\frac{(z-\bar{z})^2}{2\sigma^2}} d(z-\bar{z})$$

and of several straight lines

$$z - \bar{z} \text{ vs. } (z - \bar{z})/\sqrt{2\sigma^2}$$

for various values of  $\sigma$  (hence various values of signal to noise ratio). By means of this nomograph A and B could be read directly for many combinations of  $\bar{z}'$  and  $n$ .



SIGNAL TO NOISE POWER RATIO, S/N IN db

	a	b	c	d
B	13.0Mc/Sec.	0.182Mc/Sec.	13.0Mc/Sec.	3.32Mc/Sec.
BT	13.0	0.182	13.0	3.32

FIG. 1 SOME BETTING CURVES OF A-SCOPE EXPERIMENTS. SYSTEM PARAMETERS

$\tau = 1\mu\text{sec.}$

$s = 1.92\text{mm}/\mu\text{sec.}$

$sXT = 1.92\text{ mm}$

PRF = 200~/sec.  $T = 3.0\text{ sec.}$

PRF XT = 600 Pulses.

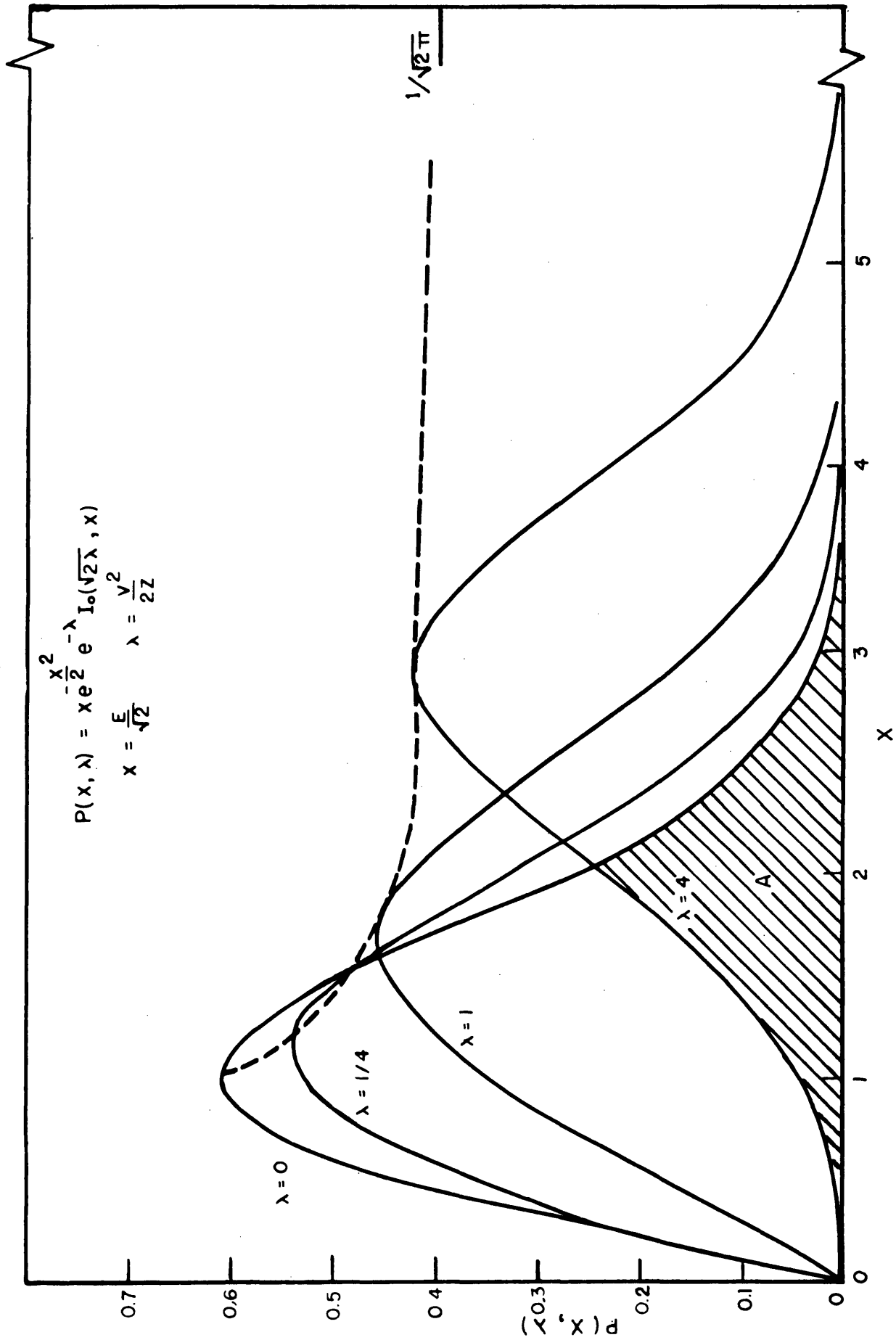


FIG. 2 - PROBABILITY DISTRIBUTION OF AMPLITUDE,  $x$ , FOR A LINEAR DETECTOR FOR NOISE, AND FOR NOISE PLUS SIGNAL

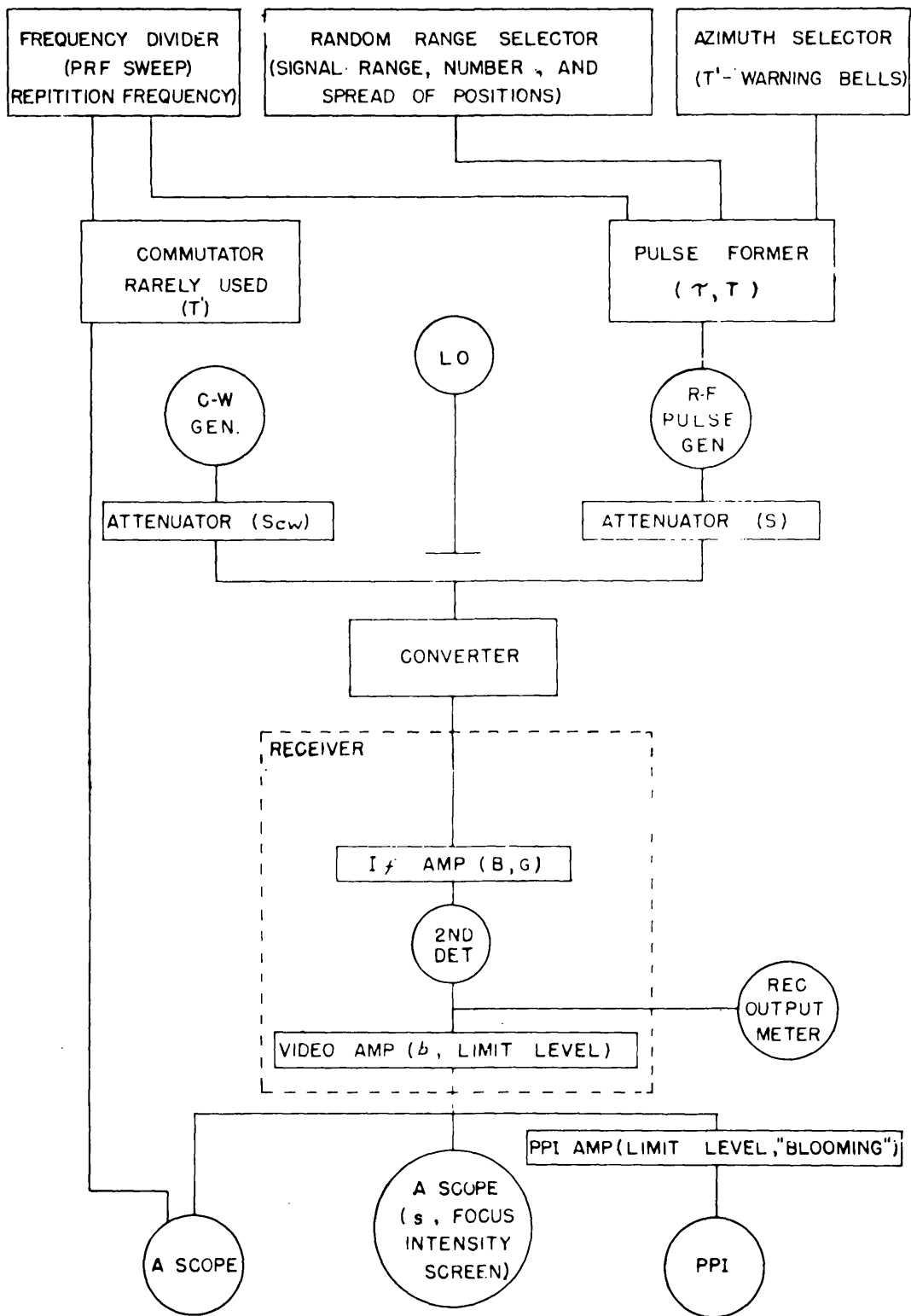


FIG. 3 BLOCK DIAGRAM OF THE SYSTEM USED FOR THRESHOLD STUDIES (PARAMETERS CONTROLLED IN EACH COMPONENT IN PARENTHESES.)

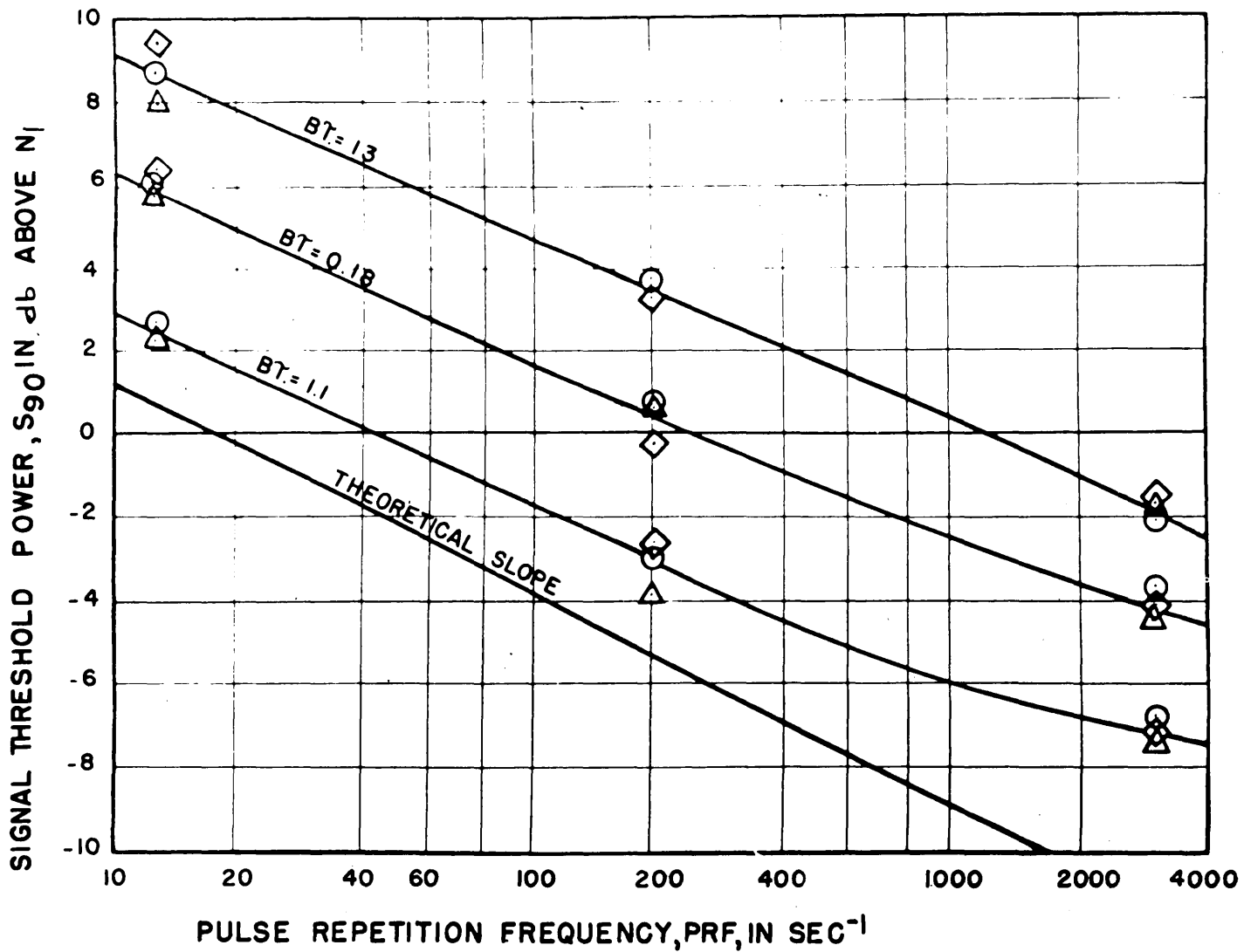


FIG.4 SIGNAL THRESHOLD POWER VS. PRF.

PULSE LENGTH	$\tau = 1\mu$ SEC.
PULSE LENGTH ON SCREEN	$5\tau = 1.7$ M.M.
VIDEO BAND WIDTH	$b = 10$ MC/SEC.
SIGNAL PRESENTATION TIME	$T = 3$ SEC.
SCOPE SCREEN	PI
$N_1 =$ NOISE POWER IN BANDWIDTH	$1.0/\tau$

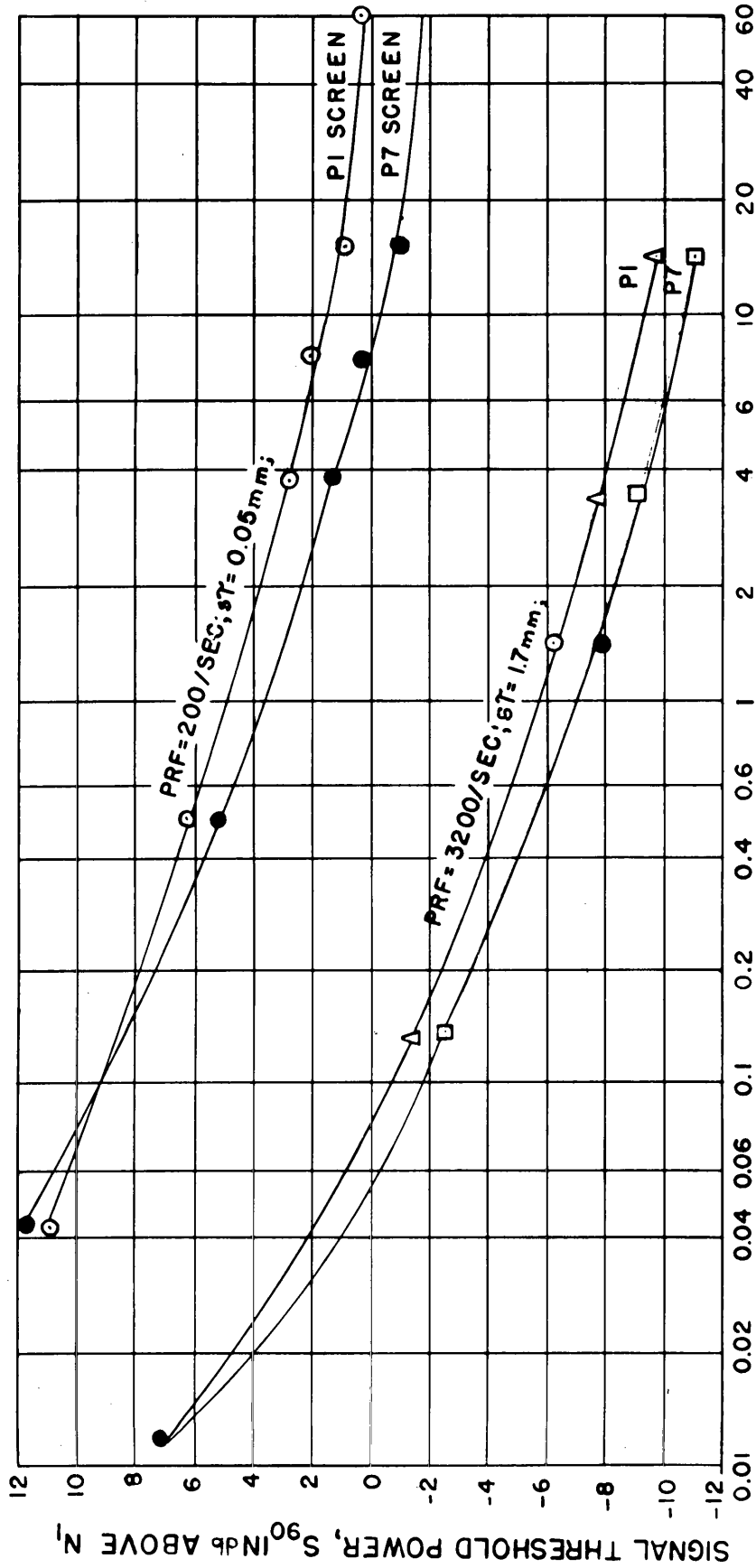


FIG. 5 SIGNAL THRESHOLD VS. SIGNAL PRESENTATION TIME

SYSTEM PARAMETERS

PULSE LENGTH  $T = 1 \mu SEC.$   
 I-F BANDWIDTH  $B = 1.14 MC/SEC.$   
 $N_1 =$  NOISE POWER IN A BANDWIDTH  $1.0/T$

OBSERVERS  
 ○ V.J.  
 ● R.A.  
 △ S.S.

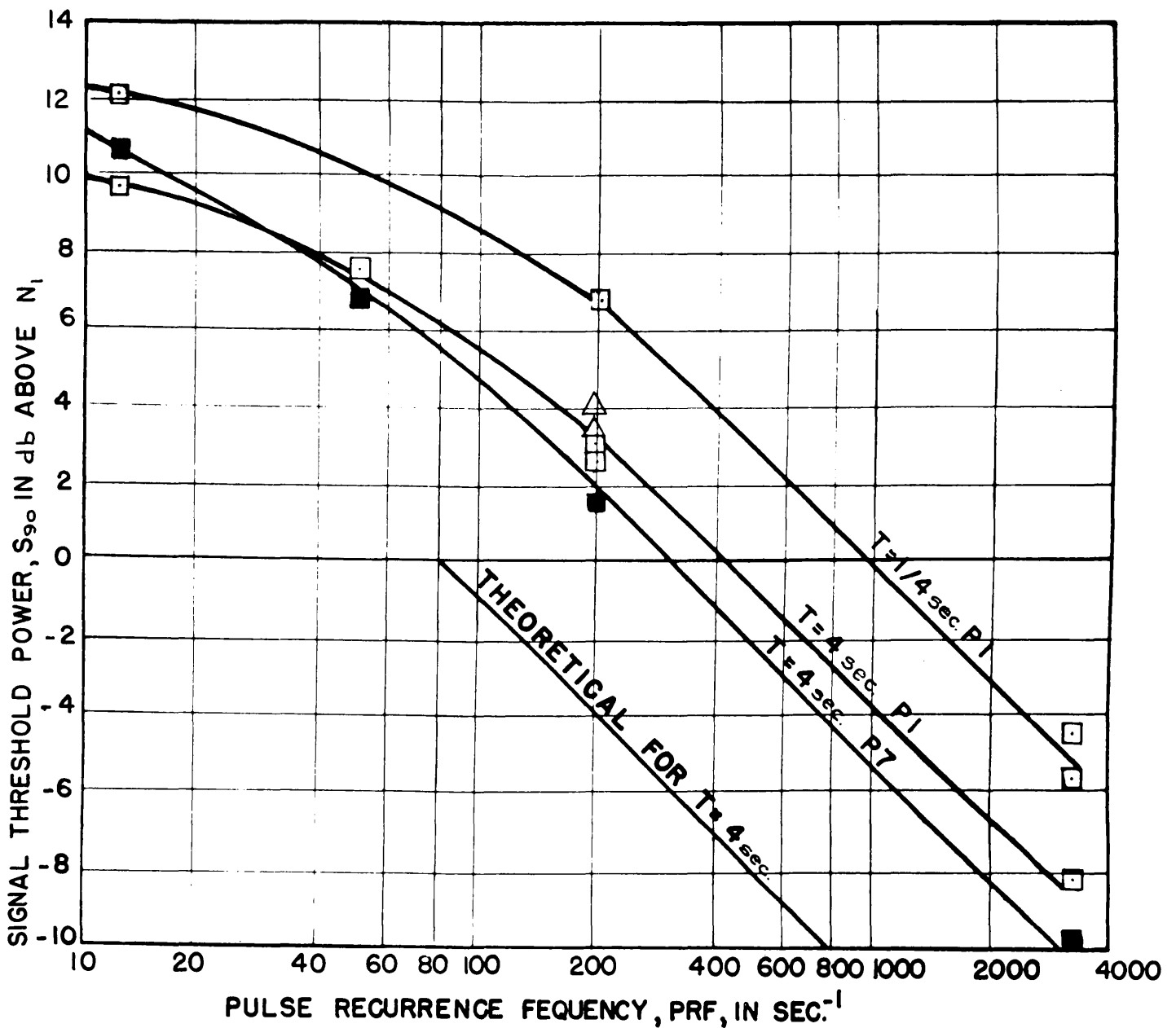


FIG.6 SIGNAL THRESHOLD VS. PULSE RECURRENCE FREQUENCY WITH SWEEP RECURRENCE FREQUENCY CONSTANT AT 3200/SEC.

SYSTEM PARAMETERS		OBSERVERS	
PULSE LENGTH	$\tau = 1 \mu \text{ sec}$	$\triangle$	R.A.
PULSE LENGTHS ON SCREEN	$s\tau = 1 \text{ mm}$	$\square$	S.S.
I.F. BANDWIDTH	$B = 1.2 \text{ Mc/sec.}$	$\blacksquare$	
$N_1 = \text{NOISE POWER IN BANDWIDTH}$	$1.0 / \tau$		

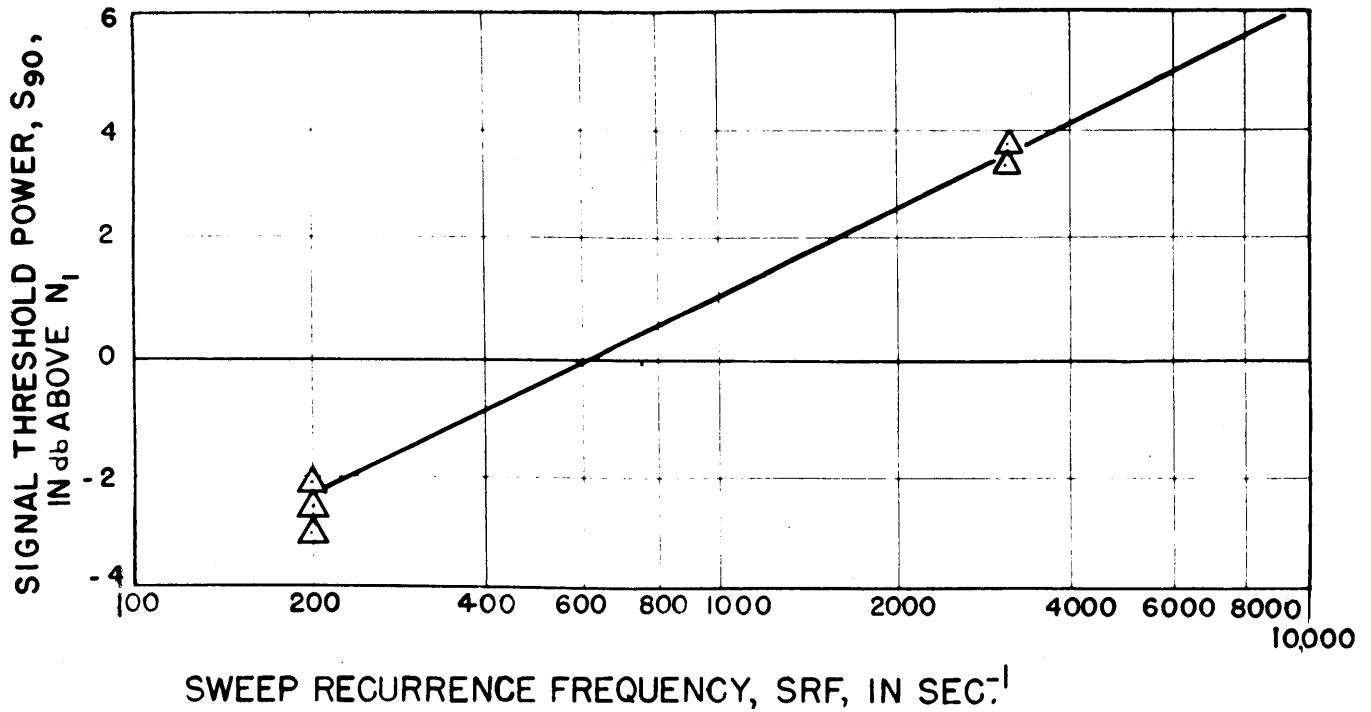


FIG. 7 SIGNAL THRESHOLD vs. SWEEP RECURRENCE FREQUENCY, SRF, WITH SWEEPS CONTAINING SIGNAL PULSE CONSTANT AT 200 PER SEC.

SYSTEM PARAMETERS

PULSE LENGTH  $\tau = 1 \mu\text{SEC.}$   
 PULSE LENGTH ON SCREEN  $s\tau = 1.7 \text{ mm}$   
 I-F BANDWIDTH  $B = 1.2 \text{ MC/SEC.}$   
 SIGNAL PRESENTATION TIME  $T = 4 \text{ SECS.}$   
 $N_i = \text{NOISE POWER IN A BANDWIDTH } 1.0/\tau$

OBSERVERS

$\Delta$  R.A.

RELATIVE SIGNAL THRESHOLD, IN dB

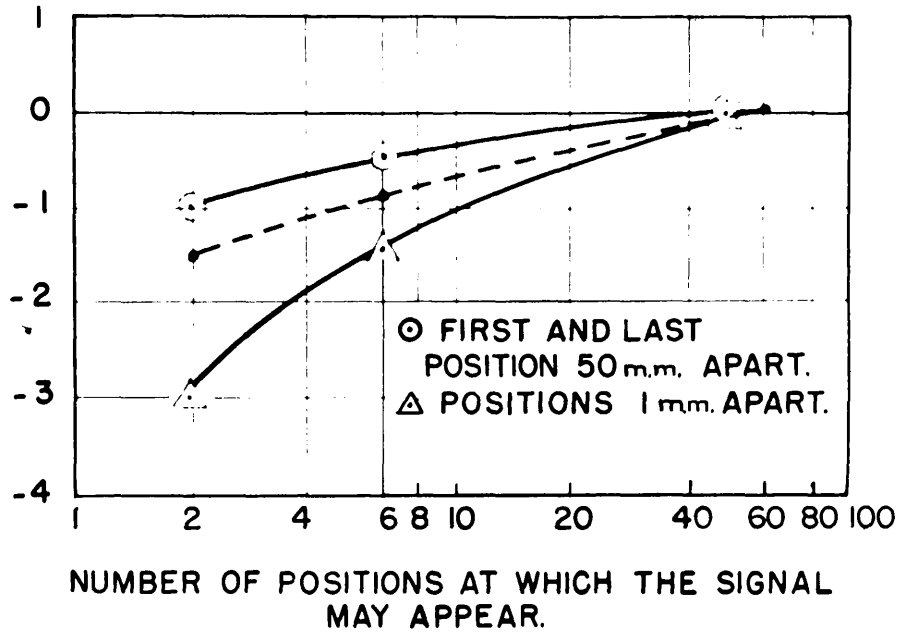


FIG.8 SIGNAL THRESHOLD VS. NUMBER OF POSSIBLE SIGNAL POSITIONS.

SYSTEM PARAMETERS

OBSERVER

$BT = 1.2$  (opt.)

○ } S.S.

$sT = 0.05$  mm

△ }

--- RELATIVE THEORETICAL DEPENDENCE

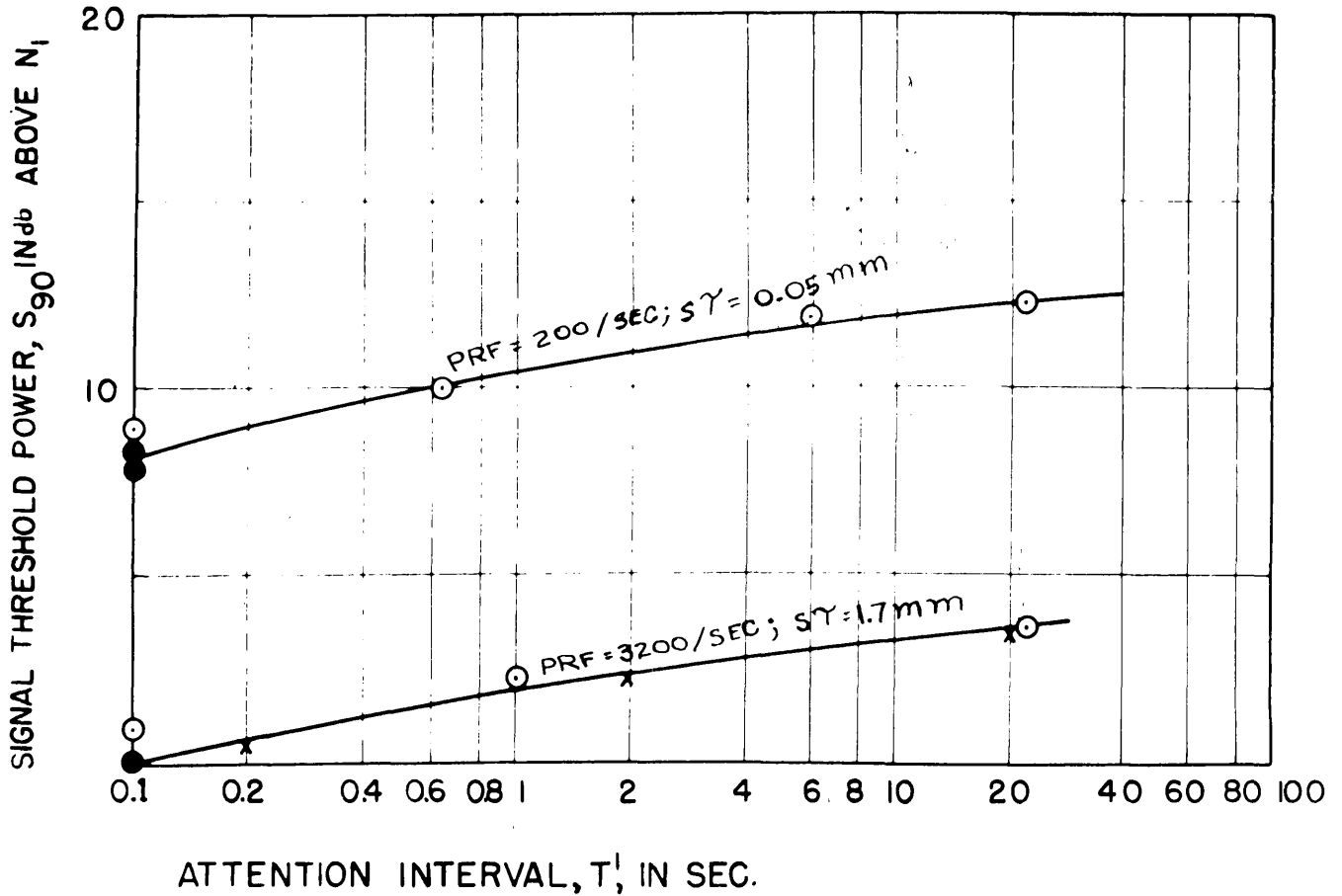


FIG.9 SIGNAL THRESHOLD VS. ATTENTION INTERVAL, WITH SIGNAL PRESENTATION TIME CONSTANT 0.1 SEC.

SYSTEM PARAMETER

$BT = 12$   
 SIGNAL PRESENTATION TIME  
 $\tau = 0.1$  SEC.  
 SCOPE SCREEN-P7  
 $N_i$  = NOISE POWER IN BANDWIDTH  $1.0/\tau$

OBSERVERS

SS ○ — BY RINGING OF BELL AT BEGINNING AND END OF INTERVAL  $T'$   
 SS ● BY TRIGGERING THE SCOPE DURING  $T'$  ONLY  
 — X — RELATIVE THEORETICAL DEPENDENCE

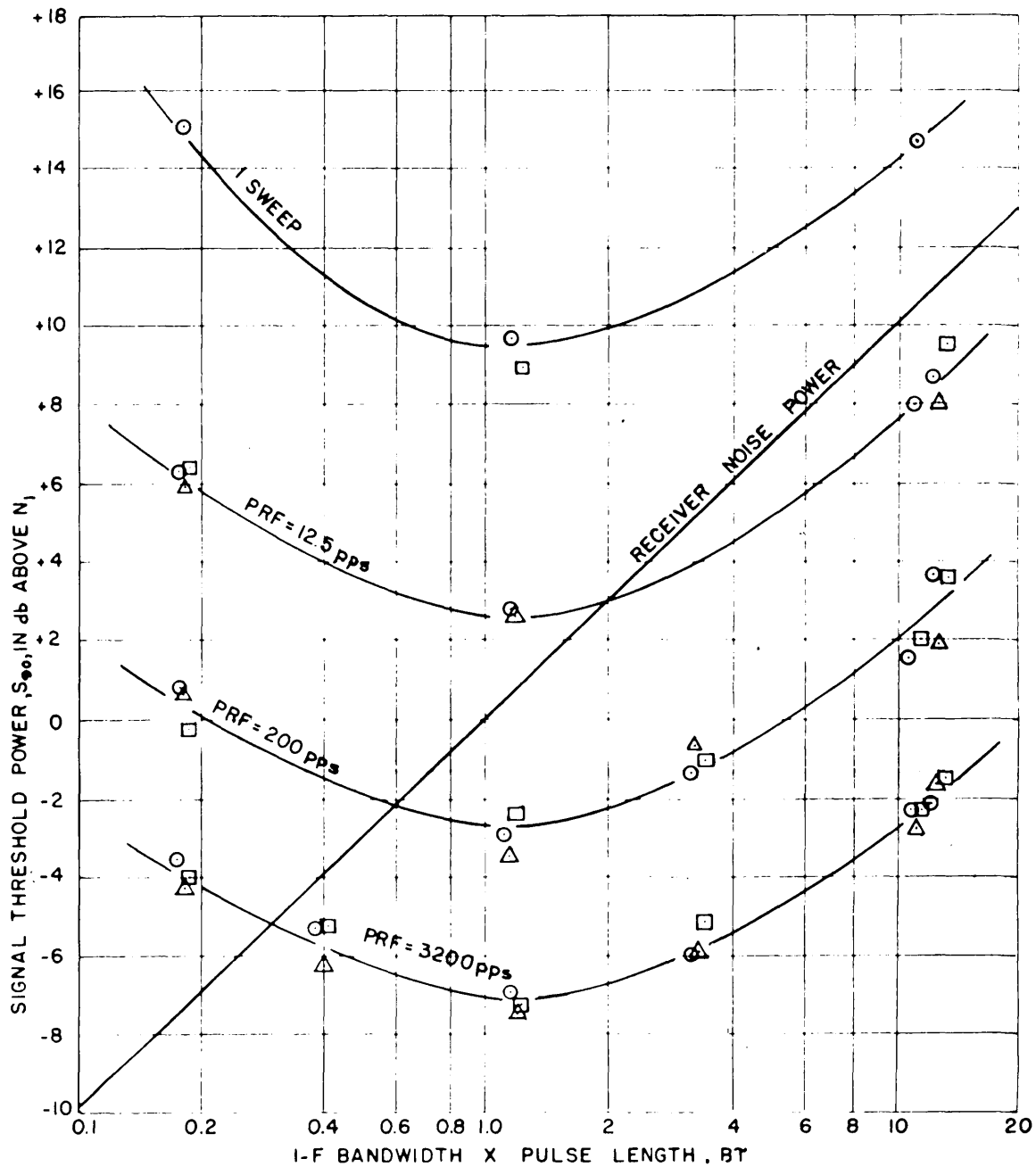


FIG.10- SIGNAL THRESHOLD POWER VS. I.F. BANDWIDTH X PULSE LENGTH.

SYSTEM PARAMETERS

PULSE LENGTH  $\tau = 1\mu \text{ sec.}$   
 PULSE LENGTH ON SCREEN  $s\tau = 1.7 \text{ mm.}$   
 VIDEO BANDWIDTH  $b = 10 \text{ Mc/sec.}$   
 SIGNAL PRESENTATION TIME  $T = 3 \text{ sec.}$   
 OSCILLOSCOPE SCREEN = PI  
 $N_1$  = NOISE POWER IN A BANDWIDTH OF  $1/T$

OBSERVERS

O R.A.  
 $\Delta$  J.L.  
 $\square$  S.S.

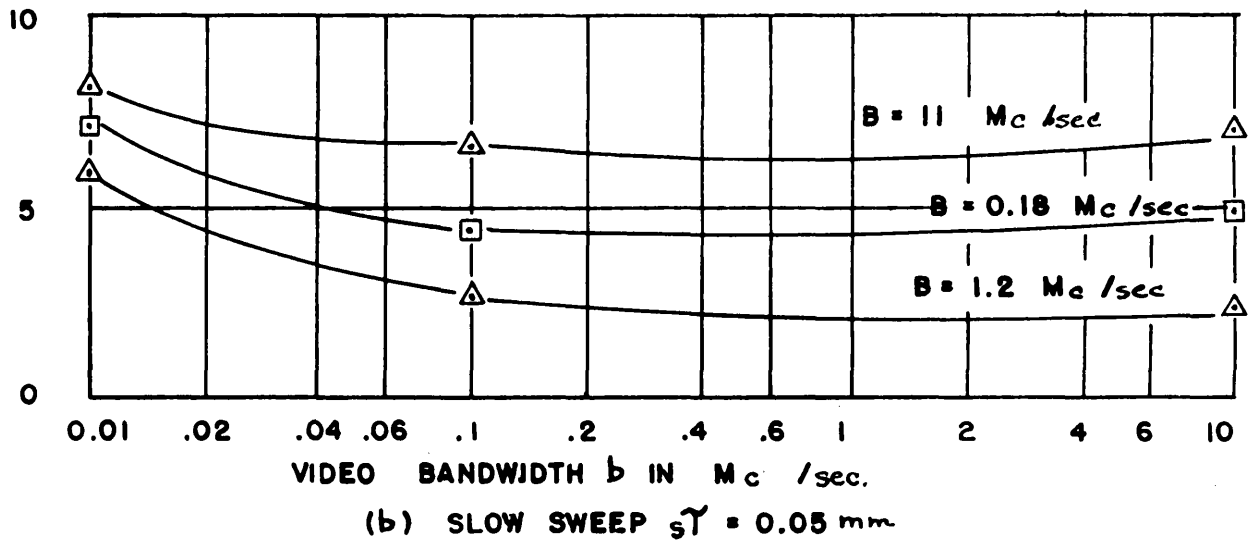
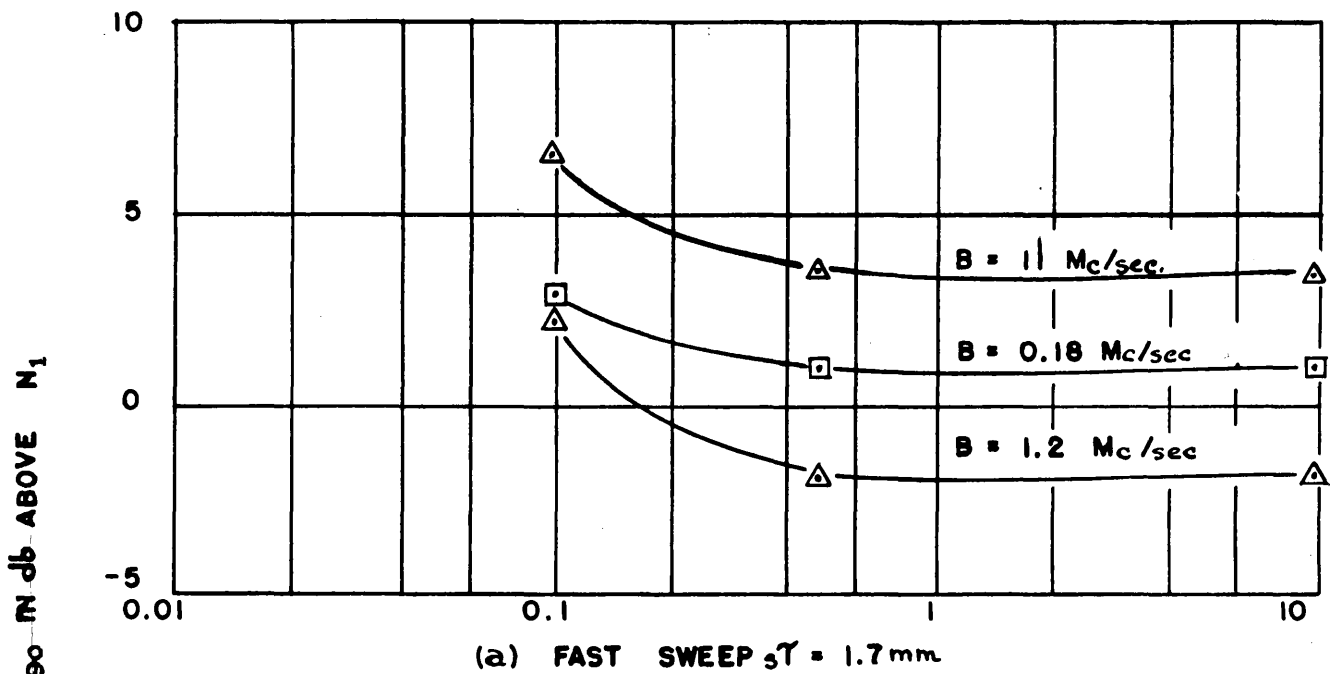


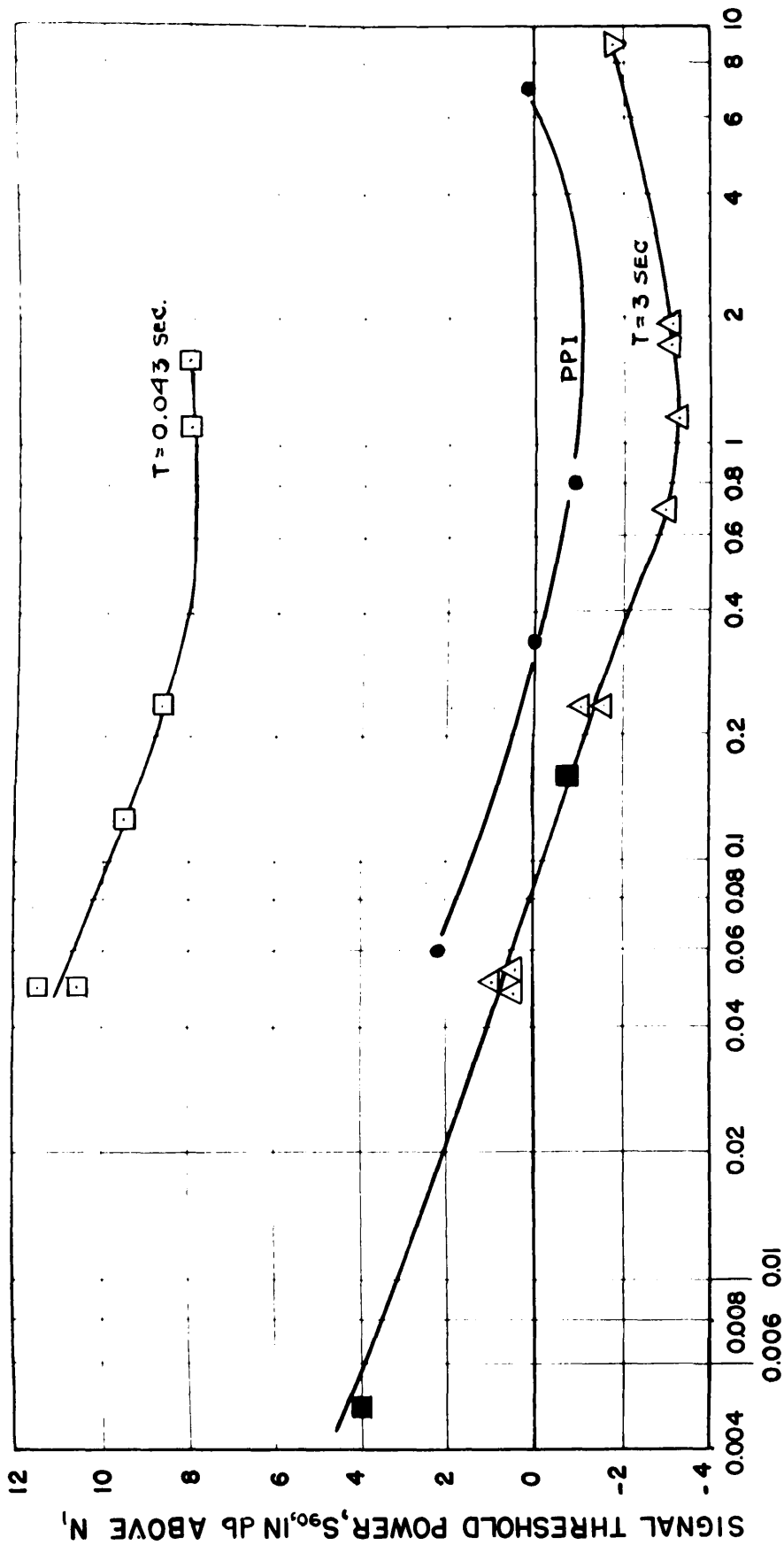
FIG. 11 SIGNAL THRESHOLD VS. VIDEO BANDWIDTH FOR FAST AND SLOW SWEEPS

SYSTEM PARAMETERS

$\tau = 1 \mu\text{sec.}$   
 $T = 3.5 \text{ sec.}$   
 $\text{PRF} = 200/\text{sec.}$   
 $\text{SCOPE SCREEN} = \text{P7}$   
 $N_1 = \text{NOISE POWER IN A BANDWIDTH } 1.0/\tau$

OBSERVER

$\Delta$  } s.s.  
 $\square$  }



PULSE LENGTH ON SCREEN,  $sT$  IN mm.

FIG.12 SIGNAL THRESHOLD VS. PULSE LENGTH ON SCREEN.

A-SCOPE SYSTEM PARAMETERS

$BT = 1.2$

PRF = 200/sec.

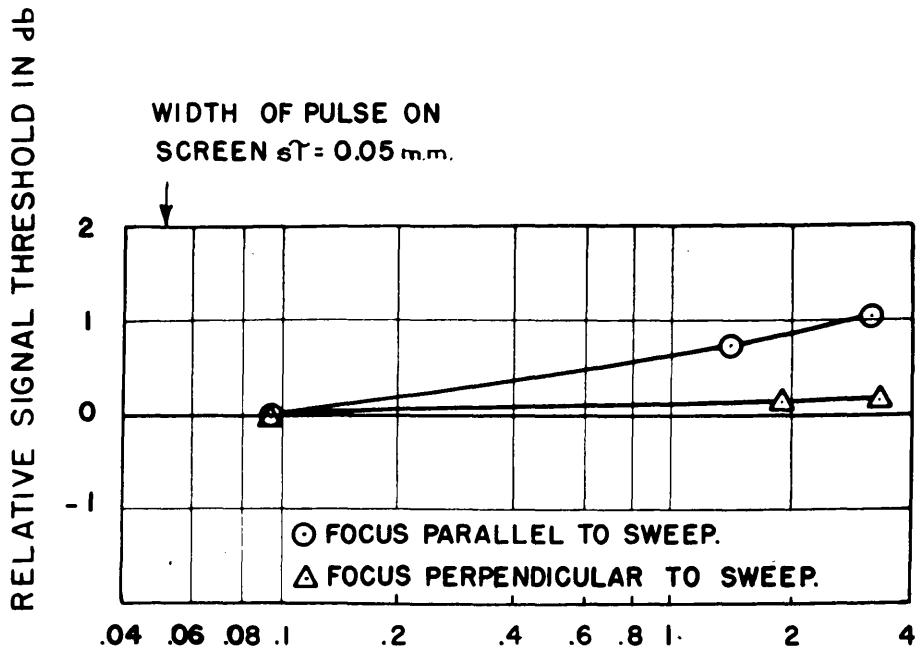
$N_1$  = NOISE POWER IN BANDWIDTH 1.0/T.

OBSERVERS

△ } R.A.

□ } S.S.

● C.M.A.  
A.G.



WIDTH OF VERTICAL OR HORIZONTAL LINES IN m.m.

FIG.13 SIGNAL THRESHOLD VS. FOCUS.

SYSTEM PARAMETERS	OBSERVER
$BT = 1.2$ (opt.)	○ } S.S.
$sT = 0.05$ m.m.	△ }
PRF = 200/sec.	
T = 3 sec.	

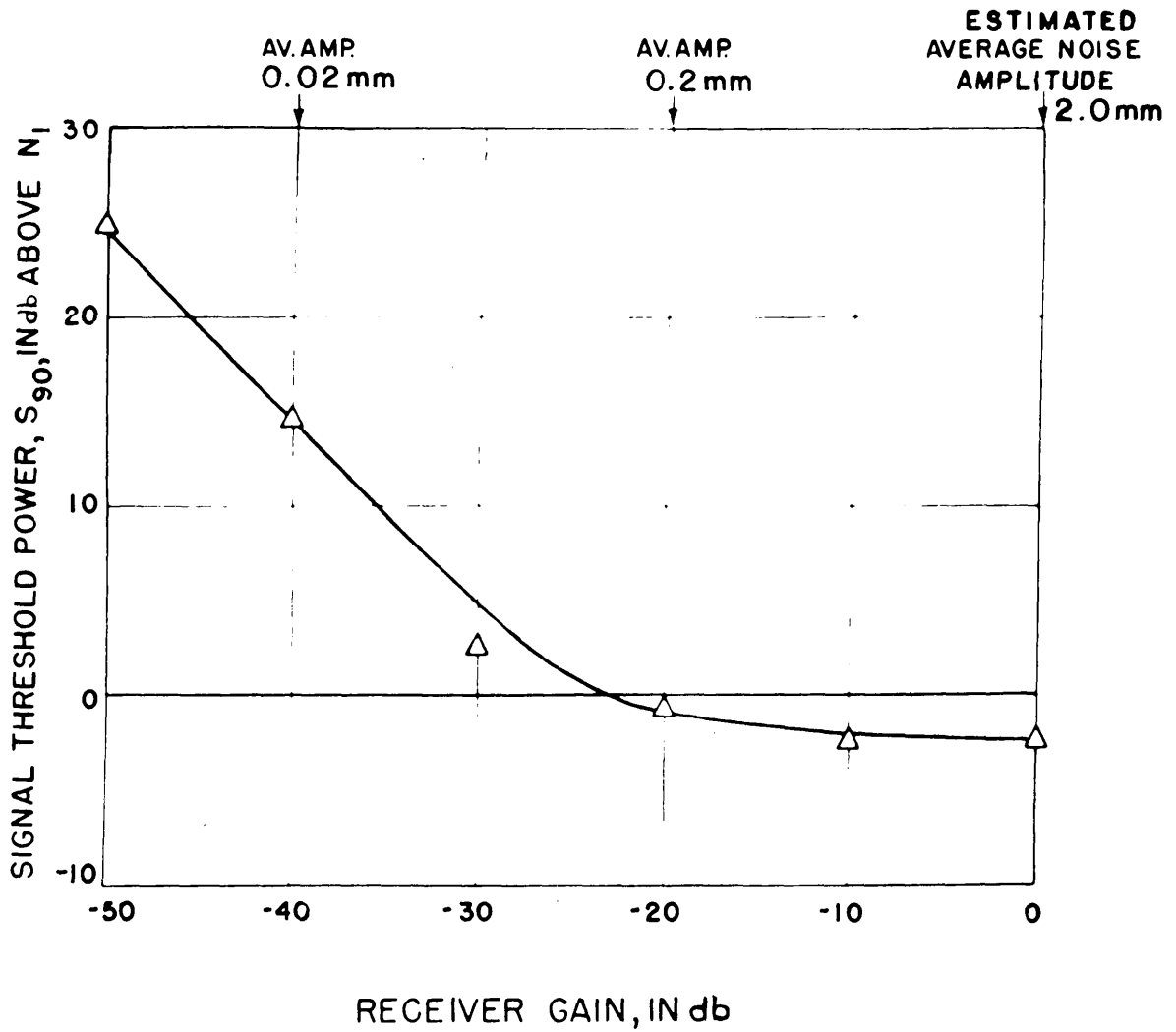


FIG.14 SIGNAL THRESHOLD vs. RECEIVER GAIN

SYSTEM PARAMETERS	OBSERVER
RT = 1.2	RA
sT = 1.7	
PRF = 200/SEC.	
T = 3.4 SEC.	
SCREEN = PI	
VIEWING DISTANCE = 30 CM	
FOCUS PERPENDICULAR TO SWEEP = 0.5 mm	
$N_1$ = NOISE POWER IN A BANDWIDTH 1.0/T	

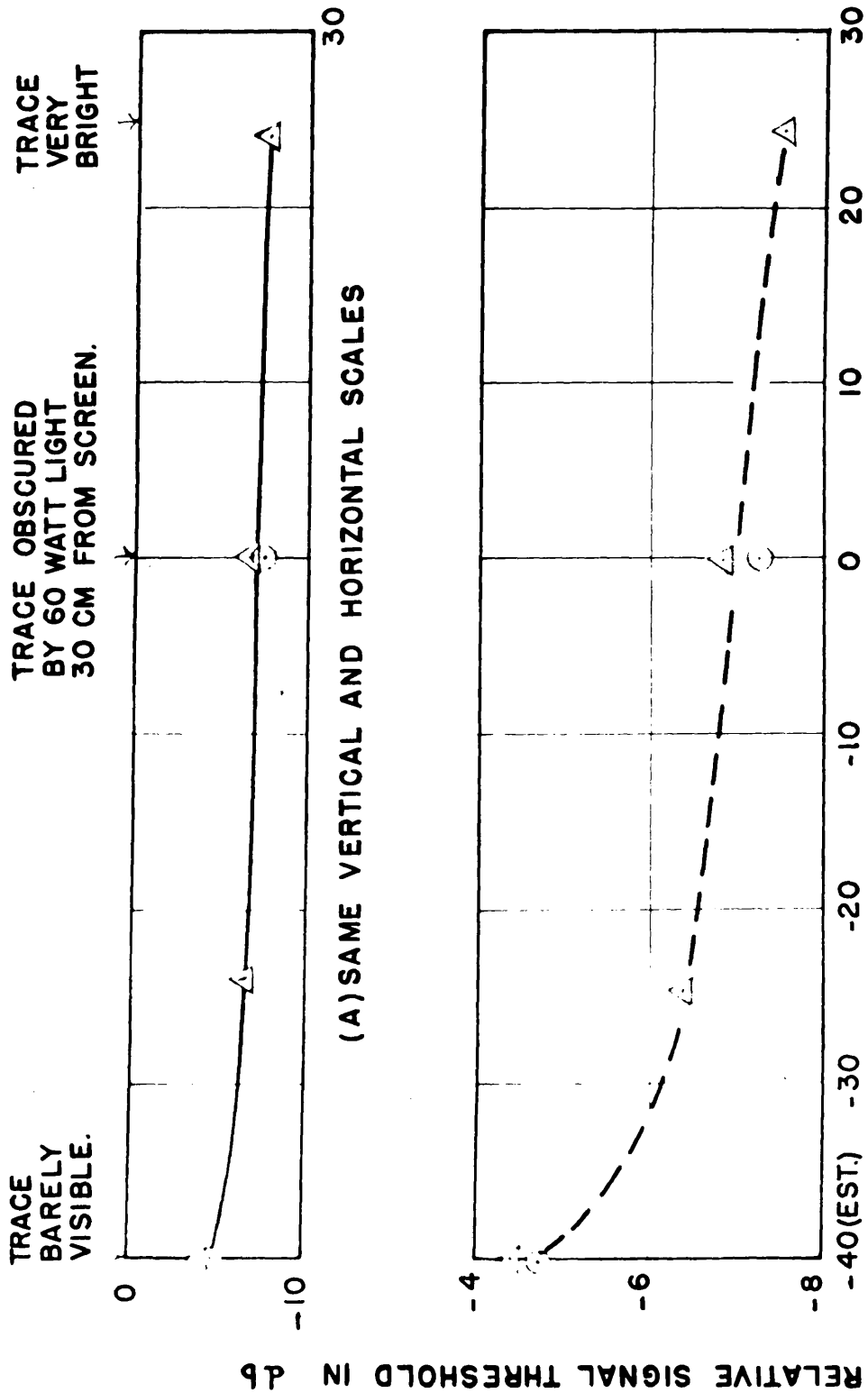


FIG. 15 SIGNAL THRESHOLD VS. TRACE INTENSITY.

SYSTEM PARAMETERS OBSERVERS SCOPE SCREEN

BT = 1.2 R.A. PI

ST = 1.7 m.m. S.S. P7

PRF = 3200/SEC.

T = 3 SEC.

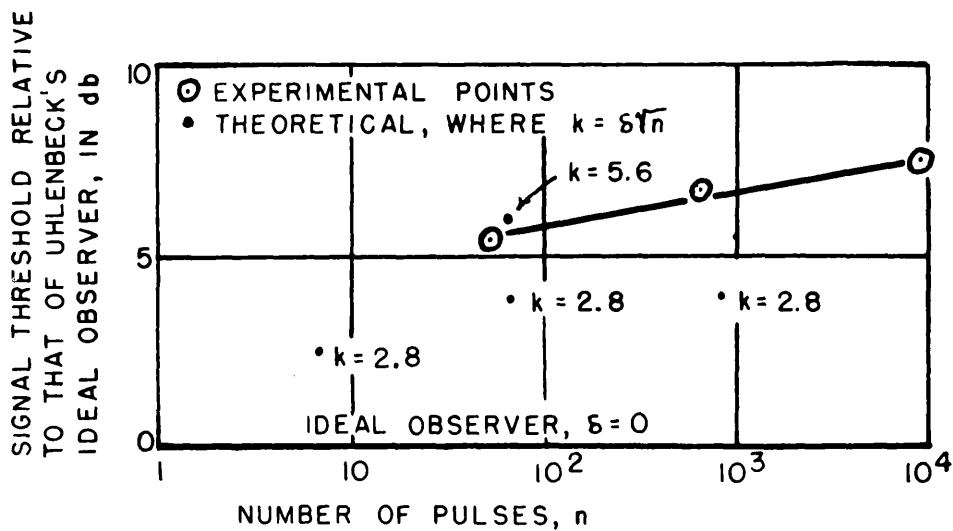


FIG. 16 - DEVIATIONS FROM THE THRESHOLD OF UHLENBECK'S IDEAL OBSERVER

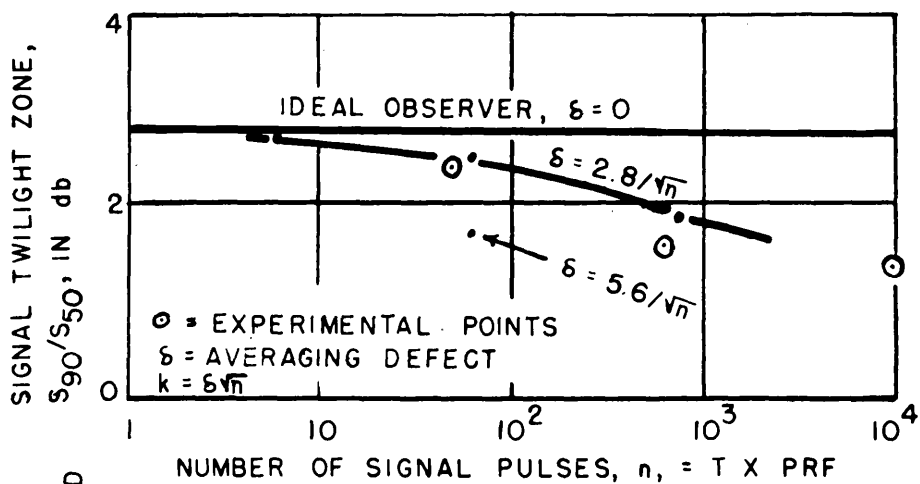


FIG. 17 - TWILIGHT ZONE VS. NUMBER OF SIGNAL PULSES

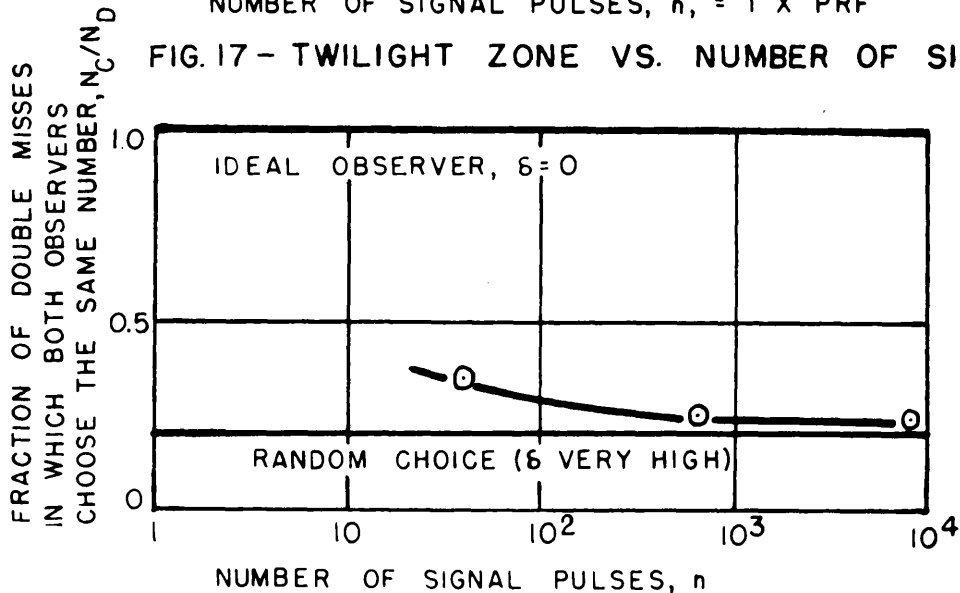
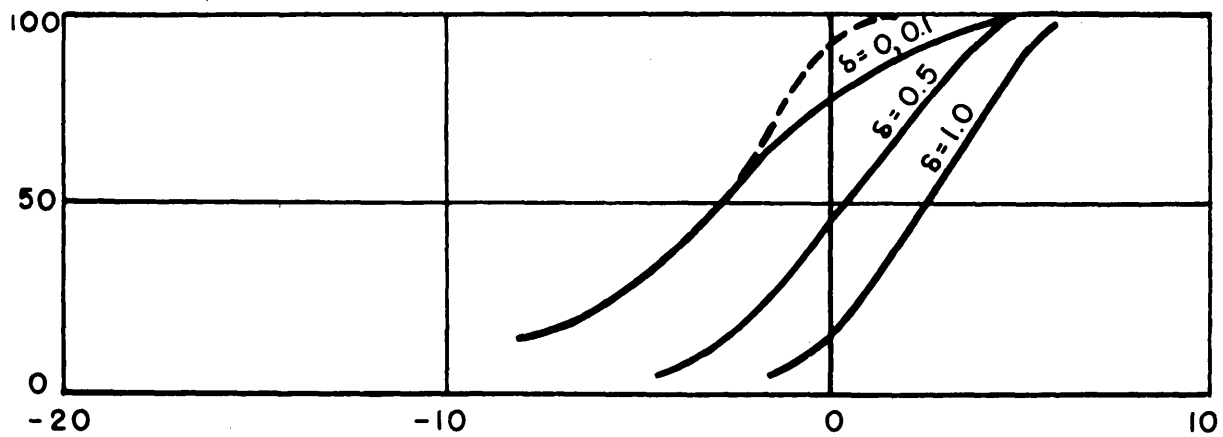
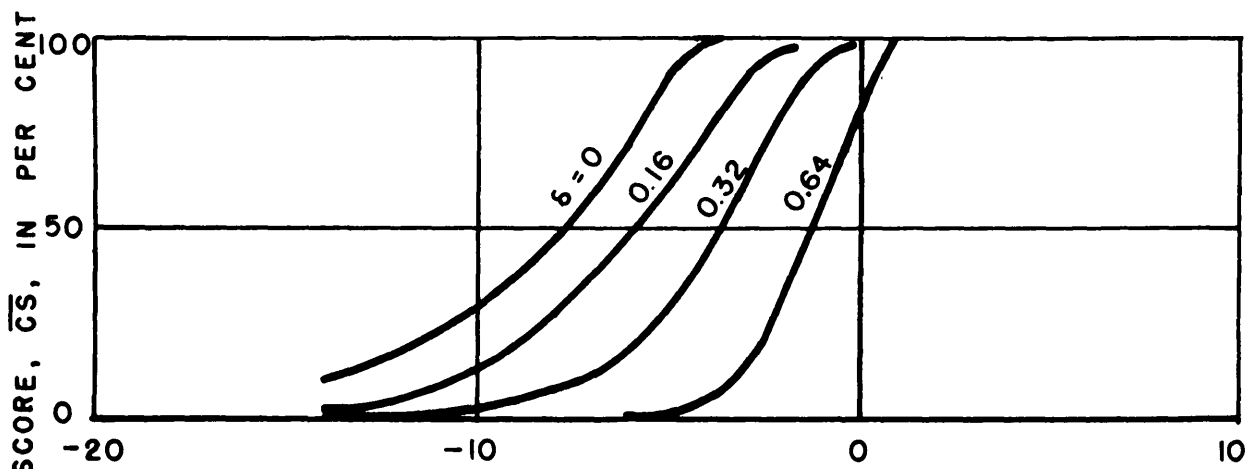


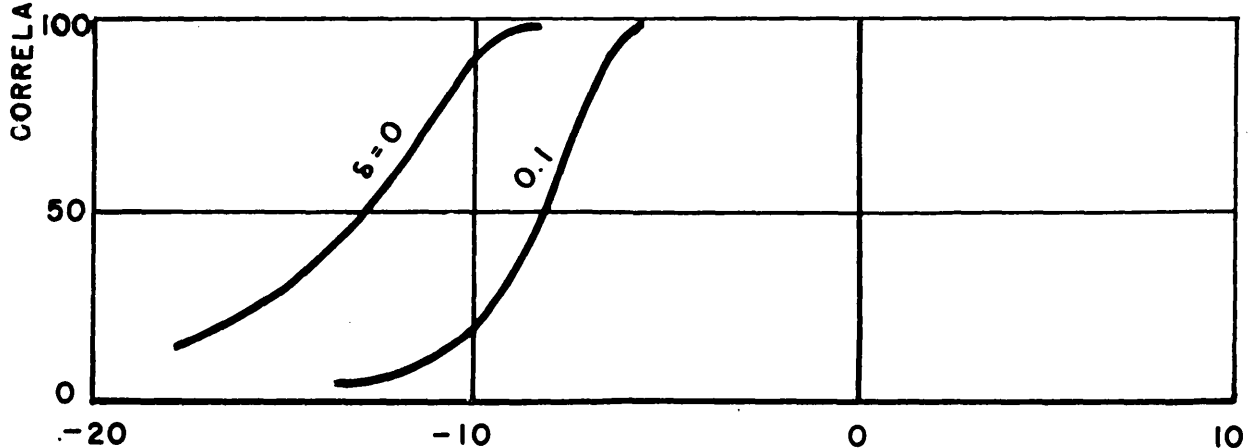
FIG. 18 - PROBABILITY OF COINCIDENT MISSES IN A 6-POSITION 2-OBSERVER EXPERIMENT



(a) 8 SIGNAL PULSES



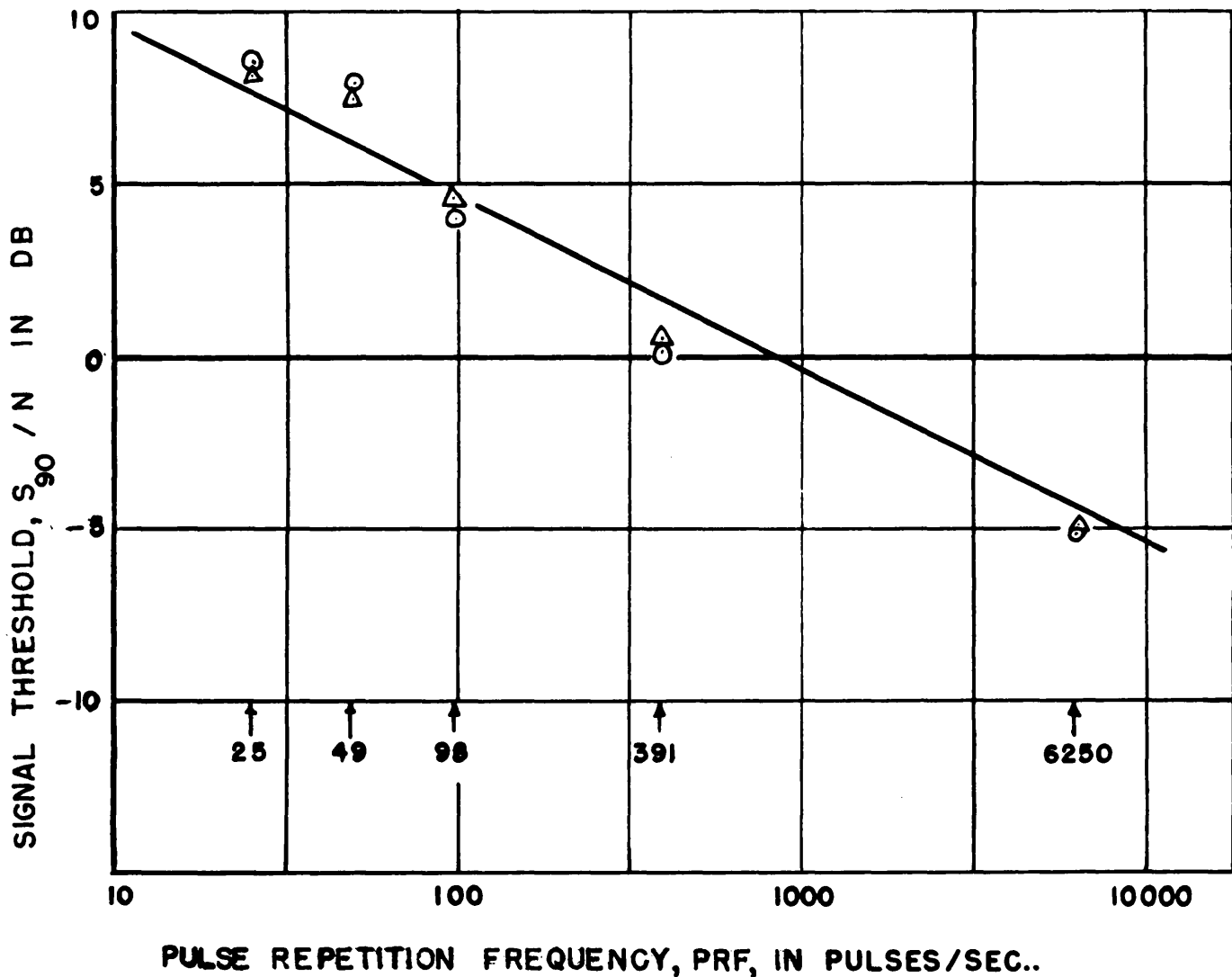
(b) 80 SIGNAL PULSES



SIGNAL TO NOISE POWER RATIO, S/N, IN db

(c) 800 SIGNAL PULSES

FIG. 19 - THEORETICAL BETTING CURVES FOR 8, 80, AND 800 SIGNAL PULSES AND VARIOUS ASSUMED VALUES OF THE AVERAGING DEFECT,  $\delta$ , OF THE OBSERVER



**SYSTEM PARAMETERS**

SIGNAL PRESENTATION TIME,  $T_s = 1/16$  sec  
 I-F BANDWIDTH,  $B_s = 1.1$  Mc/sec  
 SWEEP SPEED,  $s_s = 0.8$  mm/ $\mu$ sec  
 PULSE LENGTH,  $\gamma = 1$   $\mu$ sec

**OBSERVERS**

Δ DFG  
 ⊙ RRM

FIG. 20 - SIGNAL THRESHOLD VS. PULSE REPETITION FREQUENCY ON PPI.

BEAM ANGLE AND LENGTH OF SIGNAL ON SCOPE

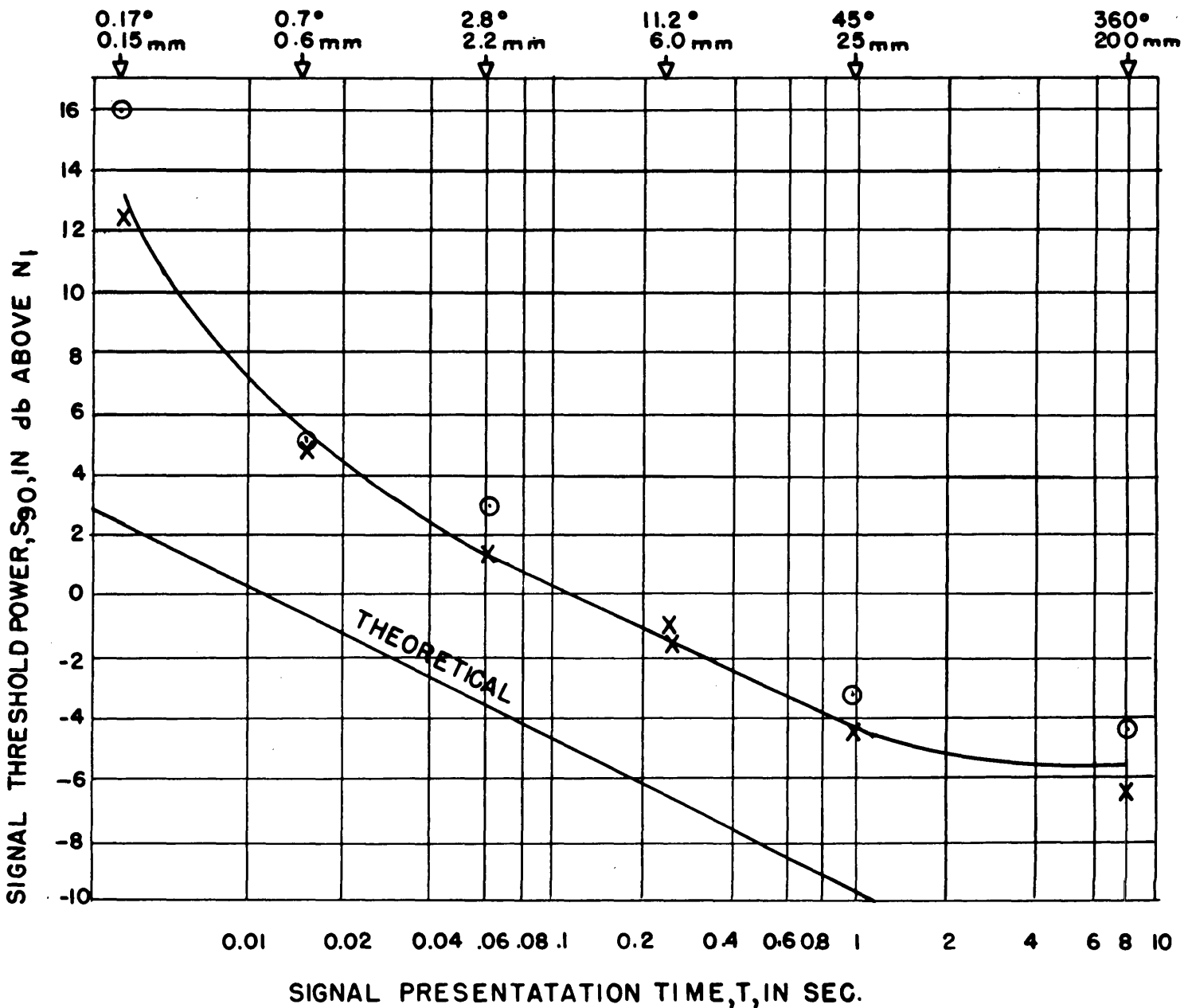


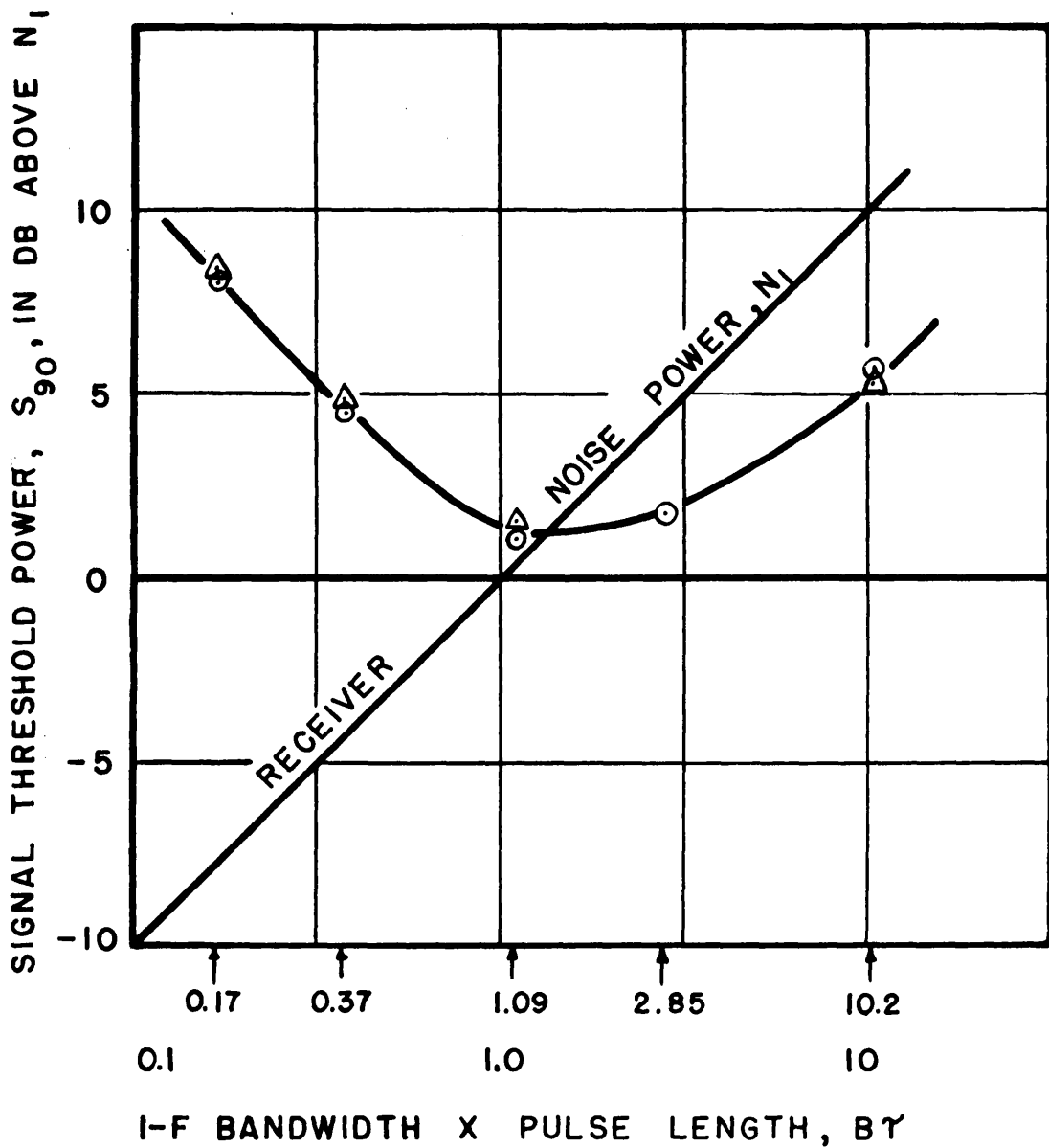
FIG.21 SIGNAL THRESHOLD VS. SIGNAL PRESENTATION TIME WITH SCANNING TIME CONSTANT.

SYSTEM PARAMETERS

PULSE LENGTH  $\tau = 1$   
 PULSE LENGTH ON SCREEN  $s\tau = 0.75$   
 I.F. BANDWIDTH  $B = 1.1$   
 P.R.F. PRF = 800/SEC.  
 $N_1 =$  NOISE POWER IN BANDWIDTH  $1.0/\tau$

OBSERVERS

O J.L.  
 X S.S.



SYSTEM PARAMETERS

PULSE REPETITION FREQUENCY, PRF, = 391 c/sec

SIGNAL PRESENTATION TIME,  $T$ , = 1/16 sec

PULSE LENGTH,  $\tau$ , = 1  $\mu$ sec

SWEEP SPEED,  $s$ , = 0.08 mm/ $\mu$ sec

$N_1$  = NOISE POWER IN BANDWIDTH 1.0/ $\tau$

OBSERVERS

$\Delta$  DFG

$\circ$  RRM

FIG. 22 - SIGNAL THRESHOLD POWER VS. I-F BANDWIDTH X PULSE LENGTH ON PPI..

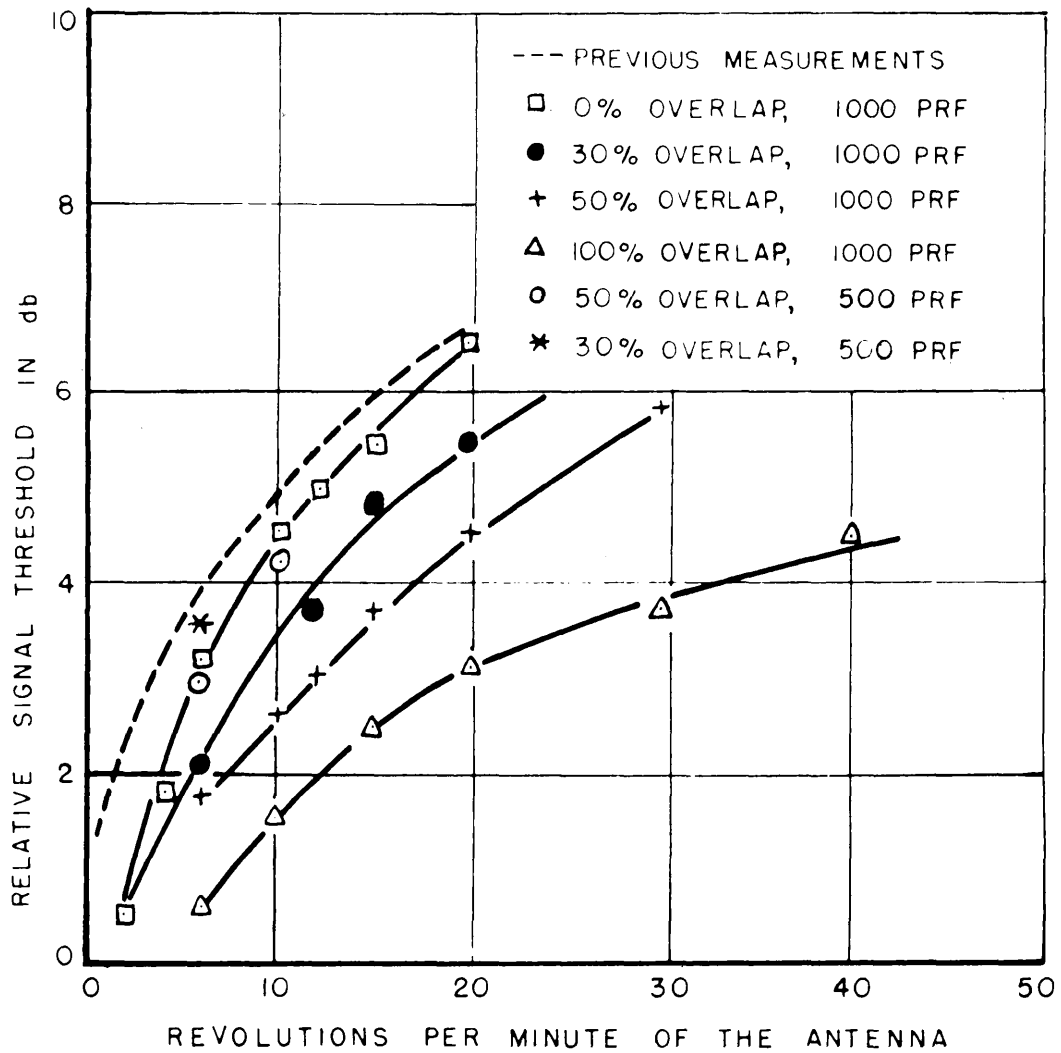


FIG. 23 - SCANNING LOSS AS A FUNCTION OF THE PER CENT OF SIGNAL OVERLAP

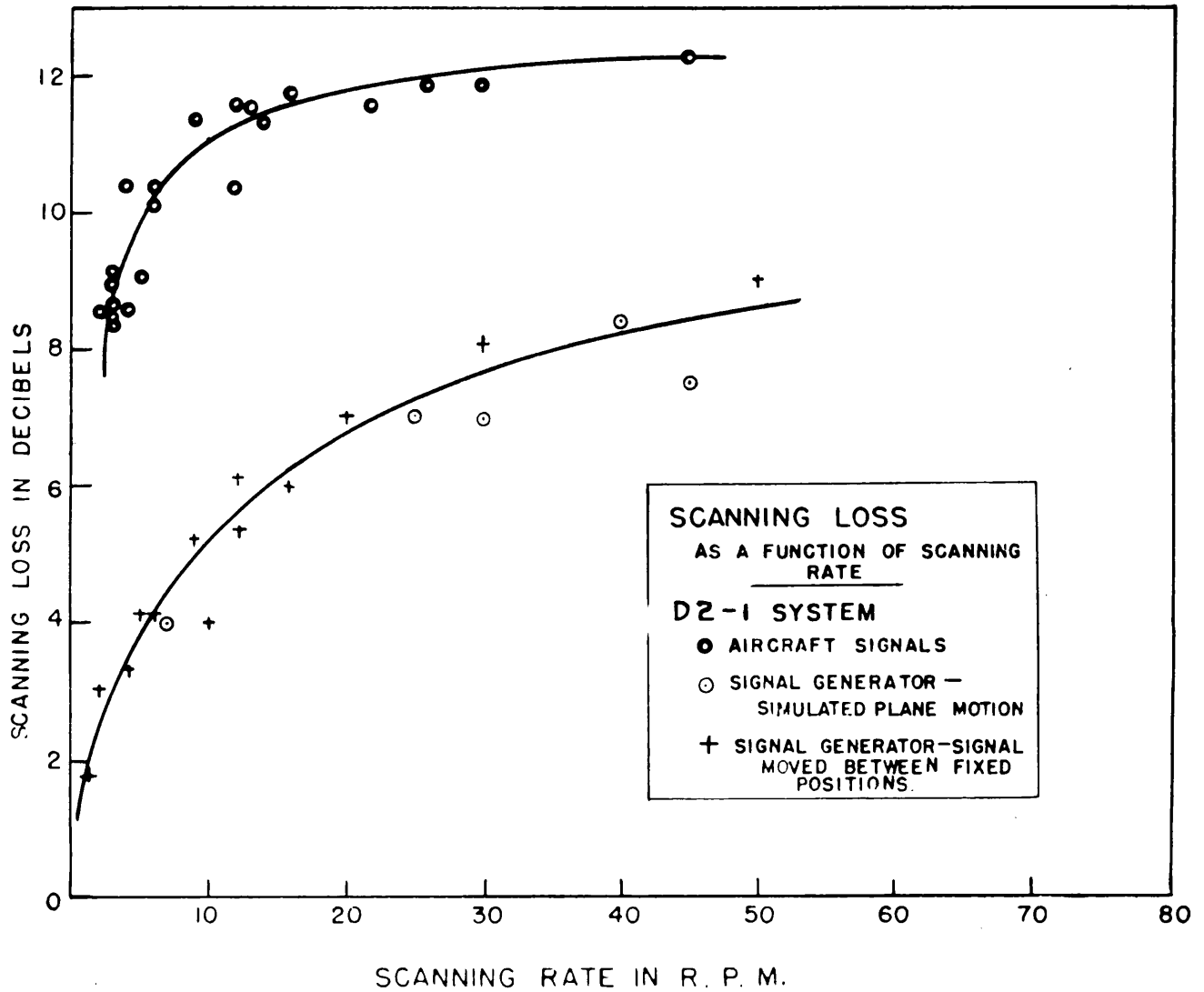


FIG. 24 SCANNING LOSS AS A FUNCTION OF SCANNING RATE

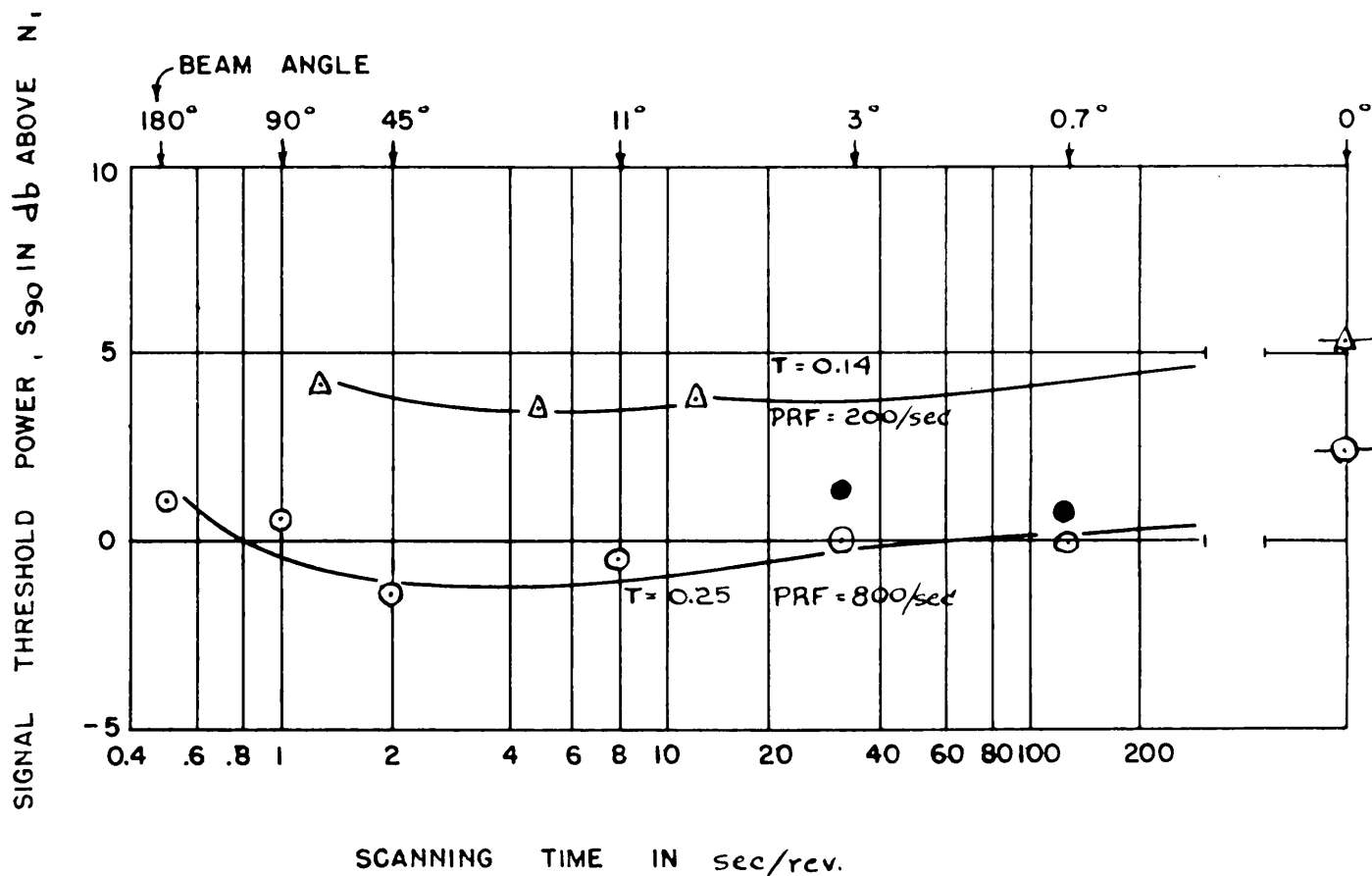
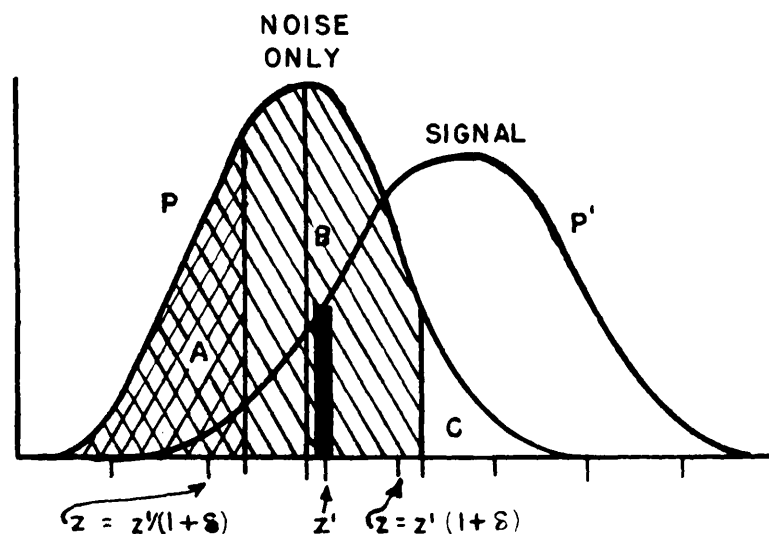


FIG. 25 SIGNAL THRESHOLD VS. SCANNING TIME WITH SIGNAL PRESENTATION TIME CONSTANT

SYSTEM PARAMETERS	OBSERVER
PULSE LENGTH $\tau = 1 \mu\text{sec}$	$\left. \begin{array}{l} \Delta \\ 0 \\ \bullet \end{array} \right\} \text{S.S.}$
PULSE LENGTH ON SCREEN $s\tau = 0.6 \text{ mm}$	
I-F BANDWIDTH $B = 1.2 \text{ Mc/sec}$	
RANGE OF SIGNALS ON SCOPE = 34 mm TO 62 mm	
$N_1 = \text{NOISE POWER IN A BANDWIDTH} - 1.0/\tau$	

PROBABILITY DENSITY, P OR P'



AVERAGE OF THE SQUARES OF THE AMPLITUDES AT A NOISE POSITION, Z, OR AT A SIGNAL POSITION, Z'

- A  OBSERVER MAKES A CORRECT STATEMENT
- B  OBSERVER GUESSES
- C  OBSERVER MAKES AN INCORRECT STATEMENT

FIG. A-1 - SCHEME FOR CALCULATING THE BETTING CURVE FOR AN OBSERVER WITH LIMITED CONTRAST DISCERNIBILITY; i.e., HAVING A FINITE AVERAGING DEFECT,  $\delta$ .